

# Estimation-Guided Guidance and Its Implementation via Sequential Monte Carlo Computation

Ilan G. Shaviv\* and Yaakov Oshman†

*Technion—Israel Institute of Technology, 32000 Haifa, Israel*

DOI: 10.2514/1.G000360

Existing missile guidance strategies are traditionally based on the separation theorem, which has never been proven valid in realistic guidance scenarios. In such cases, only the general separation theorem may be applied, implying a separately designed estimator and a guidance law accounting for the conditional probability density function. A new general-separation-theorem-compliant geometry-based approach is proposed to fusion of estimation and guidance. The conventional notion of reachability sets is extended, facilitating the introduction of miss-sets. A stochastic guidance strategy is proposed that aims at maximizing the pursuer's single-shot kill probability by driving its own miss-set to optimally cover the evader's miss-set (in a probabilistic sense). Information-based trajectory shaping is employed, when applicable, to enhance the scenario's observability, thereby reducing the evader's miss-set uncertainty. Computationally efficient sequential Monte Carlo methods are employed to estimate the evader's miss-set and implement the guidance scheme. A numerical simulation study is used to demonstrate the proposed methodology's robustness and accuracy in a realistic stochastic engagement. The performance of the proposed strategy is compared with that of an advanced perfect-information guidance law, addressing (in particular) real-time implementation issues and constraints. Proof-of-concept simulations demonstrate that the method is real-time amenable using present-day technology.

## I. Introduction

GUIDING a pursuer toward an evader has traditionally been regarded as a perfect-information deterministic problem. Most notably, guidance laws like proportional navigation and augmented proportional navigation [1], the optimal guidance law [2], and differential-game-based guidance laws [3,4] were formulated using this approach. The case of perfect but delayed information was addressed in [5]. The differential game approach was also used in [6], where information on target orientation was utilized, and in [7], which integrated the estimation delay compensated law of [5] with a time-varying game model.

In the absence of complete information, a separately designed estimator has to be incorporated to provide the missing information about the evader's state. There are many options for such an estimator, and most of them assume some knowledge about the evader's dynamic model. When this knowledge is limited, more complicated estimation tools such as multiple-model adaptive estimation [8], the interacting multiple model [9], interval Kalman filtering [10], and particle filtering [11] can be incorporated. All of these estimation methods provide some information about the conditional probability density function (PDF) of the evader's state, given the measurements. This conditional PDF is based, of course, on the knowledge the pursuer holds. In the case of particle filtering [11], the outcome of the estimator is a particle-based representation of the conditional PDF.

The practice of matching a perfect-information deterministic guidance law with a separately designed estimator (that provides this

information) in effect assumes that the separation theorem [12] is applicable. Unfortunately, as was also mentioned in [13], due to nonlinearities as well as non-Gaussian noises, this theorem has never been proven valid for realistic guidance scenarios. Moreover, many works in the field of guidance (see, e.g., [14,15]) have already pointed out the need for integration of guidance with estimation.

Based on information pattern theory, a general separation theorem (GST) was derived in [16]. The GST assumes only a causal discrete-time system (possibly nonlinear, possibly non-Gaussian), resulting in a classical information pattern [16]. Under these assumptions, the GST states that the estimator may be designed separately from the guidance law; yet, when designing the guidance law, the posterior PDF of the target's state needs to be addressed. In cases where the separation theorem is not applicable, as is the case in guidance, the GST predicts that disregarding this conditional PDF when designing the guidance law will result in degraded performance. Cases in point are [17,18], which addressed a linear problem with Gaussian noises where the separation theorem is not applicable because of an acceleration saturation. In [17], the nonlinear saturation element was replaced by a linear representation through which the conditional PDF affects the guidance. On the other hand, [18] attempted to solve the stochastic Hamilton–Jacobi–Bellman equations directly, including the nonlinear saturation effect. Either way, both papers showed that careful consideration of the conditional PDF improves performance.

A simplified and intuitive approach to the linearized Gaussian problem was presented in [19]. Expanding upon and consolidating the results of [20–22], the present paper presents a novel, unified approach to integrating guidance with estimation in a generalized nonlinear non-Gaussian framework. The new integrated estimation/guidance methodology is compliant with the GST. Furthermore, this methodology addresses the estimation needs by automatically shaping the pursuer's trajectory to improve observability. Based on the GST guideline, the proposed methodology integrates the estimated conditional PDF into the guidance algorithm. A key feature of the new methodology is the introduction of the notions of pursuer and evader miss-sets, which follow from an extension of the conventional notion of reachability set [23].

The methodology presented herein is developed in three stages. In the first stage, developed in Sec. III, a deterministic approach is taken, in the sense that the evader's state is assumed to be perfectly known. Through this approach, necessary conditions to guarantee a capture are derived, resulting in what we term the miss-set inclusion theorem. In the second stage, Sec. IV, the approach is modified to

Presented as Paper 2006-6217 at the Guidance, Navigation, and Control Conference and Exhibit, Keystone, CO, 21–24 August 2006; received 17 December 2015; revision received 13 July 2016; accepted for publication 18 July 2016; published online 6 October 2016. Copyright © 2016 by Ilan G. Shaviv and Yaakov Oshman. Published by the American Institute of Aeronautics and Astronautics, Inc., with permission. Copies of this paper may be made for personal and internal use, on condition that the copier pay the per-copy fee to the Copyright Clearance Center (CCC). All requests for copying and permission to reprint should be submitted to CCC at [www.copyright.com](http://www.copyright.com); employ the ISSN 0731-5090 (print) or 1533-3884 (online) to initiate your request.

\*Doctoral Student, Department of Aerospace Engineering; [ishaviv@gmail.com](mailto:ishaviv@gmail.com).

†Professor, Department of Aerospace Engineering; Holder of the Louis and Helen Rogow Chair in Aeronautical Engineering; [yaakov.oshman@technion.ac.il](mailto:yaakov.oshman@technion.ac.il). Fellow AIAA.

accommodate stochastic features and uncertainties due to estimation errors. By this modification, it is shown that capture cannot be guaranteed, yet the optimal guidance law is a result of a global optimization. In the last stage, Sec. V, we derive a suboptimal guidance law, termed the maximum-inclusion guidance law, which can be implemented in a feedback control configuration.

The remainder of this paper is organized as follows. The system model is defined and the problem is mathematically formulated in the next section. The underlying methodology for integrating estimation and guidance is presented and discussed in Secs. III–V. Using sequential Monte Carlo (SMC) methods [11], a numerical procedure for implementing the proposed methodology is presented in Sec. VI. A simulation study demonstrating the application of the proposed guidance methodology in a three-dimensional (3-D) nonlinear engagement scenario is presented in Sec. VII. Special attention is given to computational aspects, including real-time implementability using onboard processors and accuracy degradation due to the use of approximate Monte Carlo methods with a small number of particles. Concluding remarks are offered in the final section.

## II. Problem Formulation

A nonlinear non-Gaussian pursuer–evader interception problem is addressed. The equations of motion (EOMs) of both sides are given by

$$\dot{x}^P(t) = f^P(x^P(t), u^P(t), t), \quad u^P(t) \in U^P(t) \quad (1a)$$

$$\dot{x}^E(t) = f^E(x^E(t), u^E(t), w^E(t), t), \quad u^E(t) \in U^E(t) \quad (1b)$$

where  $x^P(t)$ ,  $u^P(t)$ , and  $U^P(t)$  are the pursuer state, control, and set of feasible controls at time  $t$ , respectively;  $x^E(t)$ ,  $u^E(t)$ , and  $U^E(t)$  are the respective evader variables at time  $t$ ; and  $w^E(t)$  is a white noise process with a known PDF  $p_{w^E}$  having a bounded support  $W^E(t)$ . The distributions of the initial states are assumed to be known and to have bounded supports. It is assumed that  $u^P(t)$  is a piecewise-constant function, being constant on time segments of length  $\Delta t$ . For simplicity, let  $t_k$  denote  $k\Delta t$  and let  $u_k^P$  denote  $u^P(t_k)$ .

It is assumed that the pursuer possesses knowledge regarding the evader's dynamics (in particular, in Sec. VII, it is assumed that the pursuer knows the evader's acceleration time constant and acceleration bounds). Although this assumption is commonplace (see, e.g., [24–26]), we assess, in Sec. VII, the sensitivity of our new methodology to this assumption, and we show that, when the pursuer has a less precise knowledge of the evader's dynamics, a graceful degradation of performance can be expected.

The pursuer acquires partial noisy measurements of the evader's state every  $\Delta t$   $s$  according to

$$z_k^P = h^P(x_k^P, x_k^E, t_k) + v_k^P \quad (2)$$

where  $v_k^P$  is the measurement noise with a known PDF. The pursuer also measures its own current state. Relative to the uncertainties in the measurements of the evader's state, these measurements may be assumed noise free. Hence, the pursuer's current state is assumed known.

Let  $\mathcal{Z}_k^P$  be the pursuer's observation history augmented with the initial conditions. Using (for example) particle filtering methodology, an estimator that generates the evader's current state conditional PDF  $p_{x_k^E|\mathcal{Z}_k^P}$  can be constructed.

The engagement termination time  $t_f$  is defined by

$$t_f \triangleq \arg \inf_{s>t} r(x^P(s), x^E(s)) \quad (3)$$

where  $r(x^P(s), x^E(s))$ , which is the distance between the evader and the pursuer at time  $s$ , is given by

$$r(x^P(s), x^E(s)) = \|L(x^P(s)) - L(x^E(s))\|_2 \quad (4)$$

In Eq. (4),  $L(x^P(s))$  and  $L(x^E(s))$  are the location coordinate vectors of the states  $x^P(s)$  and  $x^E(s)$  in 3-D space, respectively. Note that  $t_f$  is a function of the current time  $t$  because it depends on the current evader and pursuer states.

The goal of this work is to devise a feedback control law that conforms with the guidelines of the GST, i.e., of the form

$$u_k^P = \mathcal{C}(x_k^P, p_{x_k^E|\mathcal{Z}_k^P}) \quad (5)$$

that would be optimal in the sense of interception effectiveness. The best outcome for a pursuer, in a perfect-information interception engagement, is capture, which is defined by  $r(x^P(t_f), x^E(t_f)) = 0$ . Yet, as shown in Sec. IV, demanding capture in a stochastic engagement is too challenging, and a relaxed goal should be posed. The interception outcome can be defined by the single-shot kill probability (SSKP), which is a function of the miss distance and the lethality function of the warhead. To do that, we use the following simplified form for the lethality function [27]:

$$\Upsilon_{r_0}(\eta) = \begin{cases} \ell & \text{for } \eta \leq r_0 \\ 0 & \text{otherwise} \end{cases} \quad (6)$$

where  $0 < \ell \leq 1$  is the given lethality of the warhead, and  $r_0$  is the effective range of the warhead. Then, in a stochastic environment, the performance index to be maximized by the pursuer and minimized by the evader is the SSKP, given by

$$J(r_0) \triangleq \mathbb{E}[\Upsilon_{r_0}(r(x^P(t_f), x^E(t_f)))] = \ell \Pr[r(x^P(t_f), x^E(t_f)) \leq r_0] \quad (7)$$

## III. Stage 1: Deterministic Approach

The approach adopted in this section is deterministic in the sense that the evader's state is assumed to be perfectly known. Through this approach, the conditions needed to satisfy a capture of the evader by the pursuer are investigated.

Let the pursuer reachability set  $\mathcal{R}_P(x^P(t), t) \subset \mathbb{R}^3 \times \mathbb{R}^+$ , where  $\mathbb{R}^+$  denotes the real positive numbers, be the set

$$\mathcal{R}_P(x^P(t), t) \triangleq \{(L(x^P(s)), s) | x^P(s) = \Phi_{\tau=t \rightarrow s}^P(x^P(t), u^P(\tau)), s \geq t\} \quad (8)$$

for all pursuer control functions  $u^P(\tau)_{\tau=t \rightarrow s}$ , such that  $u^P(\tau) \in U^P(\tau) \forall \tau \in [t, s]$ ; and  $\Phi_{\tau=t \rightarrow s}^P(\cdot, \cdot)$  is the nonlinear state transformation from time  $t$  to time  $s$  resulting from Eq. (1a). Thus, at time  $t$ , the set of all points reachable by the pursuer from time  $t$  onward  $[\mathcal{R}_P(x^P(t), t)]$  is an extrapolation in time from a given current state  $x^P(t)$  for all possible future inputs. Notice that this definition of reachability set constitutes an extension of the common definition found in the literature (e.g., [23]) because it poses no time limit on the extrapolation.

Based on Eq. (1b), and analogous to the definition of  $\mathcal{R}_P(x^P(t), t)$ , let the evader reachability set  $\mathcal{R}_E(x^E(t), t) \subset \mathbb{R}^3 \times \mathbb{R}^+$  be defined as

$$\begin{aligned} \mathcal{R}_E(x^E(t), t) \\ \triangleq \{(L(x^E(s)), s) | x^E(s) = \Phi_{\tau=t \rightarrow s}^E(x^E(t), u^E(\tau), w^E(\tau)), s \geq t\} \end{aligned} \quad (9)$$

for all evader control functions  $u^E(\tau)_{\tau=t \rightarrow s}$ , such that  $u^E(\tau) \in U^E(\tau) \forall \tau \in [t, s]$  and all  $w^E(\tau)$  process noise realizations.

The engagement's possible outcome set at a given time  $t$  (i.e., all possible termination locations of both players in 3-D space and the associated termination times) is expressed with regard to the reachability sets by the miss-set  $\mathcal{M}(x^P(t), x^E(t), t) \subset \mathbb{R}^3 \times \mathbb{R}^+ \times \mathbb{R}^+$ , which is defined as

$$\mathcal{M}(x^P(t), x^E(t), t) \triangleq \left\{ (L(x^P(s)), L(x^E(s)), s) \mid \begin{array}{l} (L(x^P(s)), s) \in \mathcal{R}_P(x^P(t), t), \\ (L(x^E(s)), s) \in \mathcal{R}_E(x^E(t), t), \\ \text{s.t. } (x^P(s), x^E(s), s) \in \mathcal{T}, s \geq t \end{array} \right\} \quad (10)$$

where  $\mathcal{T}$  is the termination set imposed by Eq. (3). In the case of a single pass by (i.e., no second chance for the pursuer),  $\mathcal{T}$  may be defined as

$$\mathcal{T} \triangleq \left\{ (x^P(t_f), x^E(t_f), t_f) \mid \begin{array}{l} \dot{x}^P(s), \dot{x}^E(s) < 0 \quad \text{for } s < t_f, \\ \dot{x}^P(s), \dot{x}^E(s) = 0 \quad \text{for } s = t_f \end{array} \right\} \quad (11)$$

The evader and pursuer miss-sets, i.e., their terminal location sets [ $\mathcal{M}_E(x^P(t), x^E(t), t) \subset \mathbb{R}^3 \times \mathbb{R}^+$  and  $\mathcal{M}_P(x^P(t), x^E(t), t) \subset \mathbb{R}^3 \times \mathbb{R}^+$ , respectively] are defined as

$$\mathcal{M}_E(x^P(t), x^E(t), t) \triangleq \{(L(x^E(s)), s) \mid \exists x^P(s) \text{ s.t. } (L(x^P(s)), L(x^E(s)), s) \in \mathcal{M}(x^P(t), x^E(t), t), s \geq t\} \quad (12)$$

$$\mathcal{M}_P(x^P(t), x^E(t), t) \triangleq \{(L(x^P(s)), s) \mid \exists x^E(s) \text{ s.t. } (L(x^P(s)), L(x^E(s)), s) \in \mathcal{M}(x^P(t), x^E(t), t), s \geq t\} \quad (13)$$

Notice that the evader and pursuer miss-sets result from the projection of  $\mathcal{M}(x^P(t), x^E(t), t)$  onto their respective  $\mathbb{R}^3 \times \mathbb{R}^+$  spaces.  $\mathcal{M}_E(x^P(t), x^E(t), t)$  describes the evader's terminal location and the time when it is achieved in all the scenario outcomes that are possible from given  $x^P(t), x^E(t)$ , and  $t$ . The set  $\mathcal{M}_P(x^P(t), x^E(t), t)$  is defined analogously for the pursuer.

For notational conciseness, we omit in the ensuing the explicit dependence on the current state, where this does not hinder readability. In particular, we replace the notation  $\mathcal{R}_P(x^P(t), t)$  by  $\mathcal{R}_P(t)$ ,  $\mathcal{R}_E(x^E(t), t)$  by  $\mathcal{R}_E(t)$ ,  $\mathcal{M}(x^P(t), x^E(t), t)$  by  $\mathcal{M}(t)$ ,  $\mathcal{M}_P(x^P(t), x^E(t), t)$  by  $\mathcal{M}_P(t)$ , and  $\mathcal{M}_E(x^P(t), x^E(t), t)$  by  $\mathcal{M}_E(t)$ .

*Observation 1:*

$$\mathcal{M}_P(t) \subset \mathcal{R}_P(t) \quad \forall t < t_f \quad (14)$$

$$\mathcal{M}_E(t) \subset \mathcal{R}_E(t) \quad \forall t < t_f \quad (15)$$

The observation follows from noting that, in order for any point to be included in a player's terminal location set, it must be reachable by that player.

*Observation 2 (inclusion property):* The reachability sets and terminal location sets satisfy

$$\mathcal{R}_E(s) \subset \mathcal{R}_E(t) \quad \forall t < s < t_f \quad (16)$$

$$\mathcal{R}_P(s) \subset \mathcal{R}_P(t) \quad \forall t < s < t_f \quad (17)$$

$$\mathcal{M}_E(s) \subset \mathcal{M}_E(t) \quad \forall t < s < t_f \quad (18)$$

$$\mathcal{M}_P(s) \subset \mathcal{M}_P(t) \quad \forall t < s < t_f \quad (19)$$

Recalling the reachability set definition [Eq. (9)], the inclusion property for the evader results from observing that, in generating  $\mathcal{R}_E(x^E(s), s)$ , only the information (i.e., control function  $u^E$  and process noise realization  $w^E$ ) on the time interval  $[s, t_f]$  is used; whereas in generating  $\mathcal{R}_E(x^E(t), t)$ , in addition to that information, the information on the time interval  $[t, s]$  is used as well. Noting that there exists a control function that propagates the evader from state  $x^E(t)$  to  $x^E(s)$ , we conclude that any point in  $\mathcal{R}_E(x^E(s), s)$  also belongs to  $\mathcal{R}_E(x^E(t), t)$ . The converse is not true, however. To see

this, let a different control function on  $[t, s]$  propagate  $x^E(t)$  to a different evader state at time  $s$ : say,  $x^E(s)'$ . Then, as we have already shown, any point in  $\mathcal{R}_E(x^E(s)', s)$  is also in  $\mathcal{R}_E(x^E(t), t)$ . Since  $x^E(s)' \neq x^E(s)$ , then  $\mathcal{R}_E(x^E(s)', s) \neq \mathcal{R}_E(x^E(s), s)$ , which means that there exist points in  $\mathcal{R}_E(x^E(t), t)$  that do not belong to  $\mathcal{R}_E(x^E(s), s)$ . The inclusion property for  $\mathcal{R}_P(t)$ ,  $\mathcal{M}_E(t)$ , and  $\mathcal{M}_P(t)$  may be deduced by a similar reasoning. Graphically depicting the miss-set methodology to be presented in the ensuing, Fig. 1 illustrates the inclusion property stated in Observation 2. In Fig. 1, the locations at times  $t_k$  and  $t_{k+1}$  of the pursuer ( $P$ ) and evader ( $E$ ) are depicted with the resulting reachability sets and miss-sets

*Theorem 1:* A capture is guaranteed if

$$\mathcal{M}_E(t) \subset \mathcal{R}_P(t) \quad \forall t \leq t_f \quad (20)$$

*Proof:* That Eq. (20) constitutes a sufficient condition for guaranteeing a capture follows upon observing that it implies that all evader terminal locations are always reachable by the pursuer. Hence, for any evader terminal location, there exists a pursuer control function that defines a pursuer trajectory through that possible evader terminal location.  $\square$

A necessary and sufficient condition is next stated in the following theorem.

*Theorem 2:* A capture is guaranteed if, and only if,

$$\mathcal{M}_E(t) \subset \mathcal{M}_P(t) \quad \forall t \leq t_f \quad (21)$$

*Proof:* To prove sufficiency, one needs only observe that the set  $\mathcal{M}_P(t_f)$  is a singleton (i.e., all scenarios starting in a capture situation end immediately because the termination criterion is satisfied). Similarly,  $\mathcal{M}_E(t_f)$  possesses the same property. Equation (21) gives  $\mathcal{M}_E(t_f) \subset \mathcal{M}_P(t_f)$ . Because both sets are singletons, they must be identical, indicating a capture.

To prove necessity, let  $\zeta \in \mathbb{R}^3$  be any capture location. By definition, there exists a time  $T \geq t$  such that  $(\zeta, T) \in \mathcal{M}_E(t)$  and  $(\zeta, T) \in \mathcal{R}_P(T)$ . (Notice that  $T$  is the termination time for a scenario starting at the current state and having  $\zeta$  as the evader termination location.) The inclusion property (Observation 2) implies that  $(\zeta, T) \in \mathcal{R}_P(t)$ . Using Eqs. (10) and (13), we have  $(\zeta, T) \in \mathcal{M}_P(t)$ .

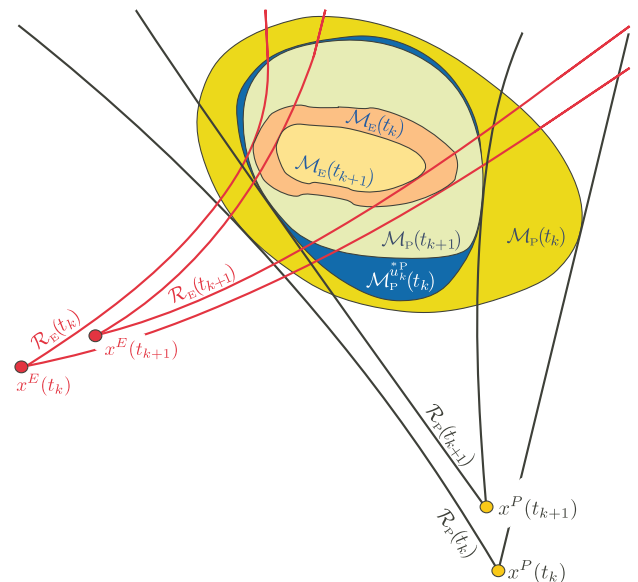


**Fig. 1** Graphical illustration of the miss-set inclusion methodology.

The theorem then follows upon recalling that  $\zeta$  is an arbitrary capture location.  $\square$

Assuming that the pursuer control function is applied at discrete times  $t_k$ ,  $k = 1 \dots \infty$ , let  $\mathcal{R}_P^y(t_k)$ ,  $\mathcal{M}^y(t_k)$ , and  $\mathcal{M}_P^y(t_k)$  be constructed in a manner similar to  $\mathcal{R}_P(t_k)$ ,  $\mathcal{M}(t_k)$ , and  $\mathcal{M}_P(t_k)$ , respectively, where the first control value in all feasible sets  $\{u_i^y\}_{i=k}^\infty$  is fixed at  $\gamma$ , i.e.,  $u^y(t_k) = \gamma$ . Then, using Theorem 2, a methodology can be derived for guaranteeing a capture. Illustrated in Fig. 1, this methodology is summarized in the following theorem.

*Theorem 3 (miss-set inclusion):* Any control function  $u_k^*P$ , selected such that

$$\mathcal{M}_P^{*P}(t_k) \supset \mathcal{M}_E(t_k) \quad \forall t_k \leq t_f \quad (22)$$

guarantees a capture.

*Proof:* By Observation 2 and by setting  $u_k^P = u_k^*P$ , it follows that

$$\mathcal{M}_E(t_{k+1}) \subset \mathcal{M}_E(t_k) \subset \mathcal{M}_P^{*P}(t_k) \quad (23)$$

Observation 1 yields

$$\mathcal{M}_P^{*P}(t_k) \subset \mathcal{R}_P^{*P}(t_k) \quad (24)$$

Noticing that  $\mathcal{R}_P^{*P}(t_k) = \mathcal{R}_P(t_{k+1})$  (Observation 2), Eqs. (23) and (24) yield

$$\mathcal{M}_E(t_{k+1}) \subset \mathcal{R}_P(t_{k+1}) \quad (25)$$

Because  $u_k^*P$  is selected such that Eq. (22) holds, Eq. (25) is satisfied for all  $k$ , hence guaranteeing capture by Theorem 1.  $\square$

Let the pursuer admissible control set be defined as

$$\mathcal{U}_P^*(t_k) \triangleq \{u_k^*P \in U^P(t_k) | \mathcal{M}_P^{*P}(t_k) \supset \mathcal{M}_E(t_k)\} \quad (26)$$

Using this definition, we next show that, under some conditions, the control function defined by Theorem 3 may not be unique, and we state these conditions.

*Observation 3:* If the closure of  $U_k^P$  is a perfect set and  $u_k^*P \in \mathcal{U}_P^*(t_k)$  satisfies

$$\partial \mathcal{M}_E(t_k) \cap \partial \mathcal{M}_P^{*P}(t_k) = \emptyset \quad (27)$$

where  $\partial S$  denotes the boundary of the set  $S$ , then  $u_k^*P$  is not unique.

To understand Observation 3, notice that each control value  $u_k^P \in U_k^P$  generates a different miss-set in the next time step. Because of Eq. (27), and the requirement that the closure of  $U_k^P$  be a perfect set, there exists a control  $\gamma \neq u_k^*P$  sufficiently close to  $u_k^*P$ , for which Eq. (27) still holds. The impact of Observation 3 is most felt when the set  $\mathcal{M}_P^{*P}(t_k)$  is much larger than the set  $\mathcal{M}_E(t_k)$ . In that case, Eq. (27) may be maintained for a wide range of controls, and the demand that the closure of  $U_k^P$  be a perfect set may be relaxed.

Observation 3 facilitates trajectory shaping. That is, because the control  $u_k^*P$  is not unique, it can be chosen from the set of controls that satisfies Theorem 3. If implemented, each of these controls will produce a different trajectory. Given a performance measure by which each of these trajectories can be rated, the optimal trajectory can be selected. Under the terms of Theorem 2, trajectory shaping has a little value, because all trajectories end in a capture, but when measurement uncertainties are introduced (as seen in the next section), this situation dramatically changes.

#### IV. Stage 2: Stochastic Guidance

To apply the proposed methodology, the reachability sets and, specifically, the miss-set  $\mathcal{M}(t_k)$  need to be estimated by the pursuer. The evader state  $x_k^E$  is not known to the pursuer, but it can be estimated by it to some degree of accuracy. Thus, the evader reachability set can

be estimated by replacing, in Eq. (9), the true state  $x_k^E$  by its estimate  $\hat{x}_k^E$ , rendering the following estimate of the evader reachability set:

$$\begin{aligned} \hat{\mathcal{R}}_E(\hat{x}^E(t_k), t_k) &\triangleq \{(L(\hat{x}^E(s)), s) | \hat{x}_k^E \sim P_{x_k^E | Z_k^P}, \\ \hat{x}^E(s) &= \Phi_{\tau=t_k \rightarrow s}^E(\hat{x}_k^E, \hat{u}^E(\tau), w^E(\tau)), s \geq t_k\} \end{aligned} \quad (28)$$

where the control process  $\hat{u}^E(\tau)_{\tau=t_k \rightarrow s}$  is defined according to prior knowledge that the pursuer holds on the evader's dynamics, either in the form of acceleration bounds or as a probabilistic model of the target acceleration command. In the latter case, the resulting set  $\hat{u}^E(\tau)$  can be regarded, for estimation needs, as a random process as well.

In much the same fashion as Eq. (10), the estimated miss-set is

$$\begin{aligned} \hat{\mathcal{M}}(t_k) &= \left\{ (L(x^P(s)), L(\hat{x}^E(s)), s) \left| \begin{array}{l} (L(x^P(s)), s) \in \mathcal{R}_P(t_k), \\ (L(\hat{x}^E(s)), s) \in \hat{\mathcal{R}}_E(t_k), \\ \text{s.t. } (x^P(s), \hat{x}^E(s), s) \in \mathcal{T}, s \geq t_k \end{array} \right. \right\} \end{aligned} \quad (29)$$

from which  $\hat{\mathcal{M}}_E(t_k)$  and  $\hat{\mathcal{M}}_P(t_k)$  are constructed in the same manner as Eqs. (12) and (13), respectively. Note that, relative to the knowledge the pursuer holds on the evader's state, its knowledge of its own state is assumed perfect; hence,  $\mathcal{R}_P(t_k)$  is assumed known in Eq. (29).

*Observation 4:* In the presence of noisy measurements, a capture cannot be guaranteed.

Noting that  $\mathcal{M}_E(t_k) \subset \hat{\mathcal{M}}_E(t_k)$ , it would seem, similarly to Theorem 2, that a capture could be guaranteed if only the condition

$$\hat{\mathcal{M}}_E(t_k) \subset \hat{\mathcal{M}}_P(t_k) \quad \forall t_k \quad (30)$$

could have been maintained. However, in contrast with Theorem 2, it is impossible to maintain Eq. (30). To see this, notice that  $\mathcal{R}_P(t_f)$  is a singleton (the pursuer knows its own location at game termination) but, due to the uncertainty in  $\hat{x}_k^E$ ,  $\hat{\mathcal{R}}_E(t_f)$  is not a singleton, i.e., the pursuer does not know the exact location of the evader. Hence, at best, Eq. (30) may be maintained up to some time  $t_G \leq t_f$ , i.e.,

$$\hat{\mathcal{M}}_E(t_k) \subset \hat{\mathcal{M}}_P(t_k) \quad \forall t_k \leq t_G < t_f \quad (31)$$

This result is a generalization of the result presented in [28], which illustrated this point in a linear problem setup for a line-of-sight rate steering missile.

By Eq. (31), it is evident that, for all  $t > t_G$ , it would be desirable to place the pursuer miss-set so that it would cover the most probable locations in which the evader terminal location may be found, i.e., the evader miss-set. To quantify this statement, the following definitions are introduced.

Define  $\Omega \triangleq \mathbb{R}^3 \times \mathbb{R}^+$ . Denote  $\mathcal{T}_E(t) \in \Omega$  and  $\mathcal{T}_P(t) \in \Omega$  as the terminal position and time pairs for the evader and pursuer, respectively, estimated by the pursuer at time  $t$ . Obviously,  $\mathcal{T}_E(t)$  is random because it depends on the future evader control function that, for the pursuer, is assumed as a random input process in addition to the process noise already assumed in the dynamics equation.

Let  $\mathcal{F}$  be a  $\sigma$ -field of subsets of  $\Omega$ , and let  $P_{\hat{\mathcal{M}}_E(t)}$  be an appropriate probability measure defined on  $\mathcal{F}$  such that  $P_{\hat{\mathcal{M}}_E(t)}(\mathcal{A})$  is the probability that, at time  $t$ , the evader terminal location is in  $\mathcal{A}$ ,  $\forall \mathcal{A} \in \mathcal{F}$ ; that is,

$$P_{\hat{\mathcal{M}}_E(t)}(\mathcal{A}) = \Pr[\mathcal{T}_E(t) \in \mathcal{A}] \quad (32)$$

The triplet  $(\Omega, \mathcal{F}, P_{\hat{\mathcal{M}}_E(t)})$  is a probability space. One possible construction for such a probability space is provided in Appendix A.

Define the guaranteed miss event, estimated by the pursuer, denoted by  $\mathcal{G}(t) \in \mathcal{F}$ , as the set of all feasible evader terminal locations that render a miss; that is,

$$\mathcal{G}(t) \triangleq \hat{\mathcal{M}}_E(t) \setminus \hat{\mathcal{M}}_P^{u^p(t)}(t) \quad (33)$$

Also, define  $\mathcal{G}^*(t)$  as the set of all feasible evader terminal locations that do not guarantee a miss; that is,

$$\mathcal{G}^*(t) \triangleq \hat{\mathcal{M}}_E(t) \cap \hat{\mathcal{M}}_P^{u^p(t)}(t) \quad (34)$$

Equations (33) and (34), and the definition of  $P_{\hat{\mathcal{M}}_E(t)}$ , yield

$$\Pr[\mathcal{T}_E(t) \in \mathcal{G}(t)] = P_{\hat{\mathcal{M}}_E(t)}(\hat{\mathcal{M}}_E(t) \setminus \hat{\mathcal{M}}_P^{u^p(t)}(t)) \quad (35a)$$

$$\Pr[\mathcal{T}_E(t) \in \mathcal{G}^*(t)] = P_{\hat{\mathcal{M}}_E(t)}(\hat{\mathcal{M}}_E(t) \cap \hat{\mathcal{M}}_P^{u^p(t)}(t)) \quad (35b)$$

It is easy to verify that  $\mathcal{G}(t)$  and  $\mathcal{G}^*(t)$  are a partition of  $\hat{\mathcal{M}}_E(t)$ , whence

$$\Pr[\mathcal{T}_E(t) \in \mathcal{G}(t)] + \Pr[\mathcal{T}_E(t) \in \mathcal{G}^*(t)] = 1 \quad (36)$$

The guaranteed miss event  $\mathcal{G}(t)$  evolves with time. It is of a particular interest to examine how  $\mathcal{G}(t)$  evolves from some past time  $s$  to the current time  $t$ . This evolution is schematically depicted in Fig. 2.

The following partition of  $\mathcal{G}(t)$  given some past time  $s$  is introduced.

*Lemma 1 (guaranteed miss-set partition):* Define  $\mathcal{G}_1(t, s)$  and  $\mathcal{G}_2(t, s)$  as

$$\mathcal{G}_1(t, s) \triangleq \hat{\mathcal{M}}_E(t) \cap \mathcal{G}(s) \quad \forall s < t \quad (37)$$

$$\mathcal{G}_2(t, s) \triangleq \hat{\mathcal{M}}_E(t) \cap \{\hat{\mathcal{M}}_P^{u^p(s)}(s) \setminus \hat{\mathcal{M}}_P^{u^p(t)}(t)\} \quad \forall s < t \quad (38)$$

Then, for all  $s < t$ ,  $\mathcal{G}_1(t, s)$  and  $\mathcal{G}_2(t, s)$  constitute a partition of  $\mathcal{G}(t)$ ; hence,

$$\mathcal{G}(t) = \mathcal{G}_1(t, s) \cup \mathcal{G}_2(t, s) \quad \forall s < t \quad (39)$$

*Proof:* The proof is provided in Appendix B.  $\square$

Applying Lemma 1 to Eq. (35a) results in

$$\Pr[\mathcal{T}_E(t) \in \mathcal{G}(t)] = \Pr[\mathcal{T}_E(t) \in \mathcal{G}_1(t, s)] + \Pr[\mathcal{T}_E(t) \in \mathcal{G}_2(t, s)] \quad \forall s < t \quad (40)$$

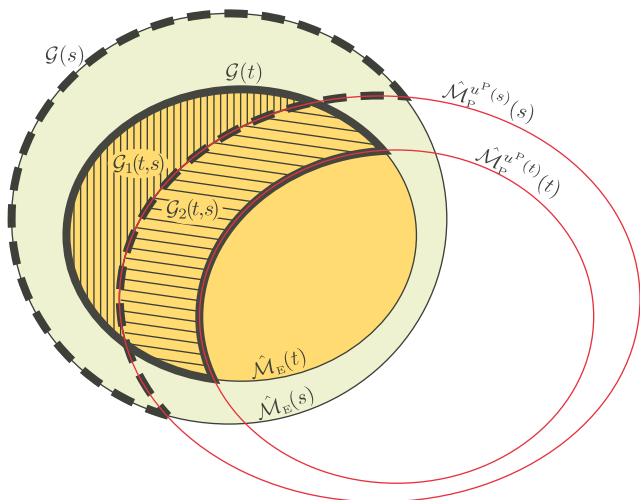


**Fig. 2** The relationship between  $\hat{\mathcal{M}}_E$  (solid fill),  $\hat{\mathcal{M}}_P^{u^p}$  (thin lines), and  $\mathcal{G}$  (thick dashed/solid line) at times  $s$  and  $t > s$ . The partition sets  $\mathcal{G}_1(t, s)$  and  $\mathcal{G}_2(t, s)$  are marked by hatch patterns.

Using the definition of  $P_{\hat{\mathcal{M}}_E(t)}$  and Eqs. (33) and (37) gives

$$\begin{aligned} \Pr[\mathcal{T}_E(t) \in \mathcal{G}_1(t, s)] &= P_{\hat{\mathcal{M}}_E(t)}(\{\hat{\mathcal{M}}_E(s) \setminus \hat{\mathcal{M}}_P^{u^p(s)}(s)\} \cap \hat{\mathcal{M}}_E(t)) \\ &= P_{\hat{\mathcal{M}}_E(t)}(\hat{\mathcal{M}}_E(s) \setminus \hat{\mathcal{M}}_P^{u^p(s)}(s)) \quad \forall s < t \end{aligned} \quad (41)$$

By the inclusion property (Observation 2), we have

$$\begin{aligned} \Pr[\mathcal{T}_E(t) \in \mathcal{G}_2(t, s)] &= P_{\hat{\mathcal{M}}_E(t)}(\hat{\mathcal{M}}_E(t) \cap \{\hat{\mathcal{M}}_P^{u^p(s)}(s) \setminus \hat{\mathcal{M}}_P^{u^p(t)}(t)\}) \\ &= P_{\hat{\mathcal{M}}_E(t)}(\hat{\mathcal{M}}_P^{u^p(s)}(s) \setminus \hat{\mathcal{M}}_P^{u^p(t)}(t)) \\ &= P_{\hat{\mathcal{M}}_E(t)}(\hat{\mathcal{M}}_P^{u^p(s)}(s)) - P_{\hat{\mathcal{M}}_E(t)}(\hat{\mathcal{M}}_P^{u^p(t)}(t)) \quad \forall s < t \end{aligned} \quad (42)$$

Notice that only  $\mathcal{G}_2(t, s)$  is affected by the pursuer control function over the time range  $(s, t]$ , whereas  $\mathcal{G}_1(t, s)$  is unaffected by the pursuer control function over this time range.

Now, let  $m_{\mathcal{G}^*}(t)$  be the estimated maximum achievable miss distance given that the evader does not guarantee a miss at time  $t$ . Thus,

$$m_{\mathcal{G}^*}(t) \triangleq \max_{\tau \geq t} \max_{\substack{(L(x^P(\tau)), \tau) \in \hat{\mathcal{M}}_P(t) \\ (L(x^E(\tau)), \tau) \in \mathcal{G}^*(t)}} r(x^P(\tau), x^E(\tau)) \quad (43)$$

The inclusion property (Observation 2) yields that

$$m_{\mathcal{G}^*}(s) \geq m_{\mathcal{G}^*}(t) \quad \forall s < t \quad (44)$$

Notice that equality in Eq. (44) holds when the evader performs the optimal evading maneuver on the time segment  $[s, t)$  and the pursuer performs the worst maneuver on the same time segment. This is due to Observation 2, which indicates that each player can control the location of its miss-set at time  $t$  within its miss-set at time  $s$  by an appropriate control function selection over this time segment.

Recalling that  $\mathcal{T}_P(t)$  and  $\mathcal{T}_E(t)$  denote the possible engagement outcomes at time  $t$  (terminal position and time for the pursuer and evader, respectively), the law of total probability gives

$$\begin{aligned} \Pr[r(\mathcal{T}_P(t), \mathcal{T}_E(t)) \leq m_{\mathcal{G}^*}(t)] &= \\ &= \Pr[r(\mathcal{T}_P(t), \mathcal{T}_E(t)) \leq m_{\mathcal{G}^*}(t) | \mathcal{T}_E(t) \in \mathcal{G}(t)] \Pr[\mathcal{T}_E(t) \in \mathcal{G}(t)] \\ &+ \Pr[r(\mathcal{T}_P(t), \mathcal{T}_E(t)) \leq m_{\mathcal{G}^*}(t) | \mathcal{T}_E(t) \in \mathcal{G}^*(t)] \Pr[\mathcal{T}_E(t) \in \mathcal{G}^*(t)] \\ &+ \Pr[r(\mathcal{T}_P(t), \mathcal{T}_E(t)) \leq m_{\mathcal{G}^*}(t) | \mathcal{T}_E(t) \notin \hat{\mathcal{M}}_E(t)] \Pr[\mathcal{T}_E(t) \notin \hat{\mathcal{M}}_E(t)] \\ &= \Pr[r(\mathcal{T}_P(t), \mathcal{T}_E(t)) \leq m_{\mathcal{G}^*}(t) | \mathcal{T}_E(t) \in \mathcal{G}(t)] \Pr[\mathcal{T}_E(t) \in \mathcal{G}(t)] \\ &+ \Pr[r(\mathcal{T}_P(t), \mathcal{T}_E(t)) \leq m_{\mathcal{G}^*}(t) | \mathcal{T}_E(t) \in \mathcal{G}^*(t)] \Pr[\mathcal{T}_E(t) \in \mathcal{G}^*(t)] \end{aligned} \quad (45)$$

where  $r(\mathcal{T}_P(t), \mathcal{T}_E(t))$  is the distance between the terminal points. The definition of  $m_{\mathcal{G}^*}(t)$  renders

$$\Pr[r(\mathcal{T}_P(t), \mathcal{T}_E(t)) \leq m_{\mathcal{G}^*}(t) | \mathcal{T}_E(t) \in \mathcal{G}^*(t)] = 1 \quad (46)$$

Hence, recalling that  $\Pr[\mathcal{T}_E(t) \in \mathcal{G}^*(t)] = P_{\hat{\mathcal{M}}_E(t)}[\mathcal{G}^*(t)]$ , Eq. (45) renders

$$\Pr[r(\mathcal{T}_P(t), \mathcal{T}_E(t)) \leq m_{\mathcal{G}^*}(t)] \geq P_{\hat{\mathcal{M}}_E(t)}[\mathcal{G}^*(t)] \quad (47)$$

Assume that  $r_0$ , the warhead effective radius defined by Eq. (6), is large enough to ensure that, at some time, denoted by  $t_\gamma$ ,

$$m_{\mathcal{G}^*}(t_\gamma) = r_0 \quad (48)$$

Using the law of total probability, Eqs. (47) and (7) yield

$$\begin{aligned}
J(r_0) &= \ell \Pr[r(\mathcal{T}_P(0), \mathcal{T}_E(0)) \leq r_0] \\
&\geq \ell \Pr[r(\mathcal{T}_P(0), \mathcal{T}_E(0)) \leq r_0 | \mathcal{T}_E(0) \in \hat{\mathcal{M}}_E(t_\gamma), \mathcal{T}_P(0) \in \hat{\mathcal{M}}_P(t_\gamma)] \times \Pr[\mathcal{T}_E(0) \in \hat{\mathcal{M}}_E(t_\gamma), \mathcal{T}_P(0) \in \hat{\mathcal{M}}_P(t_\gamma)] \\
&= \ell \Pr[r(\mathcal{T}_P(t_\gamma), \mathcal{T}_E(t_\gamma)) \leq r_0] \Pr[\mathcal{T}_E(0) \in \hat{\mathcal{M}}_E(t_\gamma), \mathcal{T}_P(0) \in \hat{\mathcal{M}}_P(t_\gamma)] \\
&\geq \ell P_{\hat{\mathcal{M}}_E(t_\gamma)}[\mathcal{G}^*(t_\gamma)] \Pr[\mathcal{T}_E(0) \in \hat{\mathcal{M}}_E(t_\gamma), \mathcal{T}_P(0) \in \hat{\mathcal{M}}_P(t_\gamma)] \\
&= \ell P_{\hat{\mathcal{M}}_E(t_\gamma)}[\mathcal{G}^*(t_\gamma)] \Pr[\mathcal{T}_E(0) \in \hat{\mathcal{M}}_E(t_\gamma) | \mathcal{T}_P(0) \in \hat{\mathcal{M}}_P(t_\gamma)] \Pr[\mathcal{T}_P(0) \in \hat{\mathcal{M}}_P(t_\gamma)] \\
&= \ell P_{\hat{\mathcal{M}}_E(t_\gamma)}[\mathcal{G}^*(t_\gamma)] P_{\hat{\mathcal{M}}_E(0)}[\hat{\mathcal{M}}_E(t_\gamma)] \Pr[\mathcal{T}_P(0) \in \hat{\mathcal{M}}_P(t_\gamma)] \tag{49}
\end{aligned}$$

where the fact that  $\hat{\mathcal{M}}_E(t_\gamma)$  is independent of  $\hat{\mathcal{M}}_P(t_\gamma)$  has been used. Notice that  $\Pr[\mathcal{T}_P(0) \in \hat{\mathcal{M}}_P(t_\gamma)] = 1$ , since the pursuer terminal position is, by definition, always within its miss-set. Also, recalling Eq. (36) renders

$$J(r_0) \geq \ell (1 - P_{\hat{\mathcal{M}}_E(t_\gamma)}[\mathcal{G}(t_\gamma)]) P_{\hat{\mathcal{M}}_E(0)}[\hat{\mathcal{M}}_E(t_\gamma)] \tag{50}$$

Analyzing Eq. (50), we notice that, at the beginning of the game, the pursuer has no control over the term  $P_{\hat{\mathcal{M}}_E(0)}[\mathcal{M}_E(t_\gamma)]$  but can only affect the value of the first term. As such, the optimal control function, in the sense of Eq. (7), can be expressed as stated in the following Theorem.

*Theorem 4:* The optimal pursuer control function, in the sense of Eq. (7), minimizes  $P_{\hat{\mathcal{M}}_E(t_\gamma)}[\mathcal{G}(t_\gamma)]$ .

Notice that, if  $r_0$  is not sufficiently large to ensure the existence of the condition expressed by Eq. (48), then

$$\lim_{t \rightarrow \infty} P_{\hat{\mathcal{M}}_E(t)}[\mathcal{G}^*(t)] = 1 \tag{51}$$

meaning a miss, almost surely.

To use Theorem 4, the pursuer needs to carry out a global optimization process. Furthermore, in order to perform this global optimization, the pursuer needs to know  $\hat{\mathcal{M}}_E(t_\gamma)$ . That is, at the start of the engagement, the pursuer needs to know the evader control function from the initial time until  $t_\gamma$ . This kind of knowledge is not readily available to the pursuer at the start of the engagement. To circumvent this difficulty, a feedback configuration guidance law, which constitutes a local optimization at each time step (and, hence, is suboptimal), is presented next.

### V. Stage 3: Maximum Inclusion Guidance Law

To implement a guidance law based on Theorem 4, a feedback configuration form of the guidance law needs to be stated first. As seen in Theorem 4, the evader's control function needs to be known. To compensate for this lack of information, we have the pursuer adopt a conservative, hence suboptimal, approach.

*Proposition 1 (maximal inclusion guidance law):* Subject to a feedback configuration form, the optimal [in the sense of Eq. (7)] pursuer control function is

$$u_k^{*P} = \arg \max_{u_k^p \in U_k^p} P_{\hat{\mathcal{M}}_E(t_k)}(\hat{\mathcal{M}}_P^{u_k^p}(t_k)) \tag{52}$$

*Proof:* First, notice that, if  $\hat{\mathcal{M}}_E(t_k) \subset \hat{\mathcal{M}}_P^{u_k^p}(t_k)$ , then  $P_{\hat{\mathcal{M}}_E(t_k)}(\hat{\mathcal{M}}_P^{u_k^p}(t_k)) = 1$ , whence Proposition 1 degenerates to Theorem 3 (miss-set inclusion), thereby proving that Proposition 1 is a more general form of the guidance law.

Recalling Eq. (50), and since  $J(r_0) \leq \ell$  from Eq. (7), maximizing the lower bound will ensure a maximal SSKP for the pursuer. Also, noticing that  $P_{\hat{\mathcal{M}}_E(0)}(\hat{\mathcal{M}}_E(t_\gamma))$  does not depend on the pursuer's actions yields that minimizing  $P_{\hat{\mathcal{M}}_E(t_\gamma)}(\mathcal{G}(t_\gamma))$  means maximizing the SSKP. The pursuer is to achieve this goal through a series of decisions separately made at each time step. Recalling Eq. (39), we have that, over the time segment  $(t_{k-1}, t_k]$ , the guaranteed miss-set  $\mathcal{G}(t_k)$  is composed of the following two subsets: 1)  $\mathcal{G}_1(t_{k-1}, t_k)$ , which

is solely affected by the evader control function over the time segment  $(t_{k-1}, t_k]$ ; and 2)  $\mathcal{G}_2(t_{k-1}, t_k)$ , which is the only subset of the guaranteed miss event,  $\mathcal{G}(t_k)$ , the pursuer can affect by the choice of its control function. Adopting a conservative approach, the pursuer assumes that the evader acts to maximize  $P_{\hat{\mathcal{M}}_E(t_k)}(\mathcal{G}_1(t_{k-1}, t_k))$ . This approach resembles the differential game approach, in which each player applies the optimal, from its own perspective, guidance law, whereby any deviation from it serves its opponent's benefit. To minimize  $P_{\hat{\mathcal{M}}_E(t_k)}(\mathcal{G}(t_k))$ , the pursuer is to select its control function by

$$\begin{aligned}
u_k^{*P} &= \arg \min_{u_k^p \in U_k^p} P_{\hat{\mathcal{M}}_E(t_k)}(\mathcal{G}(t_k)) \\
&= \arg \min_{u_k^p \in U_k^p} \{P_{\hat{\mathcal{M}}_E(t_k)}(\mathcal{G}_1(t_{k-1}, t_k)) + P_{\hat{\mathcal{M}}_E(t_k)}(\mathcal{G}_2(t_{k-1}, t_k))\} \\
&= \arg \min_{u_k^p \in U_k^p} \{P_{\hat{\mathcal{M}}_E(t_k)}(\mathcal{G}_2(t_{k-1}, t_k))\} \\
&= \arg \min_{u_k^p \in U_k^p} \{P_{\hat{\mathcal{M}}_E(t_k)}(\hat{\mathcal{M}}_P^{u_k^p}(t_{k-1})) - P_{\hat{\mathcal{M}}_E(t_k)}(\hat{\mathcal{M}}_P^{u_k^p}(t_k))\} \tag{53}
\end{aligned}$$

where we have used the fact that

$$P_{\hat{\mathcal{M}}_E(t_k)}(\hat{\mathcal{M}}_E(t_k) \cap A) = P_{\hat{\mathcal{M}}_E(t_k)}(A) \quad \forall A \subset \mathbb{R}^3 \times \mathbb{R}^+ \tag{54}$$

The proposition follows from noticing that only  $P_{\hat{\mathcal{M}}_E(t_k)}(\hat{\mathcal{M}}_P^{u_k^p}(t_k))$  is affected by the choice of  $u_k^p$ .  $\square$

Notice that the guidance law of Proposition 1 is only suboptimal in the global sense of Eq. (7), as there is no guarantee that the global minimum value of  $P_{\hat{\mathcal{M}}_E(t_\gamma)}(\mathcal{G}(t_\gamma))$  is reached through this steepest descent approach.

### VI. Guidance Law Implementation

Theorem 2 states the conditions under which a hit can be guaranteed in perfect-information cases where only the general separation theorem is applicable, e.g., the case of nonlinear dynamics and non-Gaussian process noises. In contrast, in the case of partial information, a hit cannot be guaranteed (see Theorem 4), and a suboptimal guidance law is stated in Proposition 1. Furthermore, Observation 3 indicates that the guidance law is nonunique, thus facilitating trajectory shaping. The ensemble of these elements provides the foundation for the proposed implementation approach for guiding a pursuer toward an evader in the presence of partial information, nonlinear dynamics, and non-Gaussian noises.

The proposed approach comprises the following steps:

1) The posterior density  $p_{x_k^e | z_k^p}$  is constructed using a particle filter [11].

2) The set of admissible control functions  $\mathcal{U}_p^*(t_k)$ , which satisfies Theorem 3 with  $\mathcal{M}(t_k)$  replaced by  $\hat{\mathcal{M}}(t_k)$ , is determined using a sequential Monte Carlo method (presented next).

3) If  $\mathcal{U}_p^*(t_k) \neq \emptyset$ , the control function is selected by complying with an additional constraint. Two such possible constraints are presented in the following, with each shaping the pursuer trajectory in a different manner.

4) If  $\mathcal{U}_p^*(t_k) = \emptyset$ , the control function is found according to Proposition 1.

These steps are detailed in the ensuing.

### A. Determination of $\mathcal{U}_p^*(t_k)$

Since each of the two miss-sets is represented by a set of particles, it is extremely difficult to determine if the inclusion property holds. Due to this difficulty, the procedure detailed in the following attempts to directly determine if  $\gamma \in \mathcal{U}_p^*(t_k)$ .

In the case of missile guidance, and assuming that the control is the missile acceleration perpendicular to the velocity vector, we have  $\gamma \triangleq [a_1^c(t_k), a_2^c(t_k)]^T$ , which is the immediate time step acceleration command. The following definition and assumptions are applicable:

*Definition 1 (time-invariant control set):* Define the pursuer time-invariant control set as

$$u^p(\tau) = \delta, \quad \forall \tau \geq t \quad (55)$$

where  $\delta \in U^p(\tau)$  is a constant.

Again, in missile guidance, we have  $\delta \triangleq [a_1^c, a_2^c]^T$ , which are the two time-invariant acceleration commands perpendicular to the velocity vector.

If the feasible control set  $U^p(t)$  is not time invariant, then a time-invariant control function should be stated by factors on the feasible control values at each time. For example, in a scalar example where  $U^p(t) = [u^{\min}(t), u^{\max}(t)]$ , redefine the control function to be  $\delta(t) \in [0, 1]$ , where the actual control function value is then given by  $u^p(t) = u^{\min}(t) + \delta(t)(u^{\max}(t) - u^{\min}(t))$ . In this case, a time-invariant control function set is defined as  $\delta(t) = \delta = \text{const}$ .

*Observation 5:* Assuming an acceleration control function, any point in  $\mathcal{R}_p(t)$  is reachable by a time-invariant control set, provided that the pursuer location is a smooth function of  $u^p(t)$  and the closure of  $U^p(t)$  is a perfect and convex set for all  $k$ .

Observation 5 results from the fact that all points on the boundary of the set  $\mathcal{R}_p(t)$  are achieved by having the control function fixed at an extremal admissible value. For example, if  $u^p(t)$  is scalar, then the admissible set of control function is the interval  $U^p(t) = [u^{\min}, u^{\max}]$  and the reachable set  $\mathcal{R}_p(t)$  lies on a hyperplane in  $\mathbb{R}^3 \times \mathbb{R}^+$  (since there is only one degree of freedom to control the location of the pursuer). Setting  $u^p(t) = u^{\min}$  for all  $t$  results in a trajectory along one boundary of the set  $\mathcal{R}_p(t)$ , whereas setting  $u^p(t) = u^{\max}$  for all  $t$  results in a trajectory along the other boundary of the set  $\mathcal{R}_p(t)$ . Since the closure of  $U_k^p$  is perfect and convex, any time-invariant control function set between  $u^{\min}$  and  $u^{\max}$  is feasible. Furthermore, since the system equation [Eq. (1a)] is continuous with respect to  $u^p(t)$ , all time-invariant control function sets between  $u^{\min}$  and  $u^{\max}$  result in a trajectory between the two formerly stated trajectories.

The direct procedure attempts to find, for each evader particle, a possible pursuer future control set that would cause the pursuer to intercept that evader particle. Define the pursuer front corresponding to time  $t_k$  as

$$\mathcal{F}_k(s, \gamma) \triangleq \{L(x^p(s)) | (L(x^p(s)), s) \in \mathcal{R}_p^y(t_k)\} \quad (56)$$

and propagate it simultaneously to the propagation of the evader particles. Notice that  $\mathcal{F}_k(s, \gamma)$  describes a surface in  $\mathbb{R}^3$  that evolves with time for  $s \geq t_k$ . The procedure seeks the impact locations of all evader particles on the front. Specifically, let  $\kappa_j(\gamma)$  be the location where the trajectory of the  $j$ th evader particle intercepts the front  $\mathcal{F}_k(s, \gamma)$ . From Observation 5, any point on the front  $\mathcal{F}_k(s, \gamma)$  is reachable by a pursuer control function of the form

$$u_i^p = C_k(\gamma, \delta) \triangleq \begin{cases} \gamma & \text{for } i = k \\ \delta & \text{for } i > k \end{cases} \quad (57)$$

Thus, for every  $\kappa_j(\gamma)$ , there is a matching  $\delta_j(\gamma)$  such that a pursuer driven by a control function  $C_k(\gamma, \delta_j(\gamma))$  will hit  $\kappa_j(\gamma)$ . This procedure is illustrated graphically in Fig. 3.

The front surface is extended, at its edges, by a surface that is set to be tangent to the front. Let  $I(C_k(\gamma, \delta))$  be an indicator function defined as

$$I(C_k(\gamma, \delta)) \triangleq \begin{cases} 1 & \delta \in U_i^p, i \geq k + 1 \\ 0 & \text{otherwise} \end{cases} \quad (58)$$

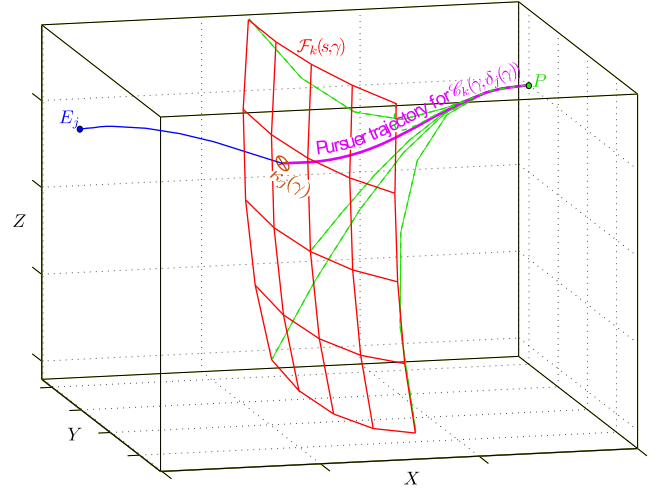


**Fig. 3** Illustration of the front procedure, showing the impact location of evader particle  $j$  with the front, the corresponding pursuer trajectory, and the pursuer extremal trajectories.

If it is feasible for the pursuer to reach the impact locations of all evader particles, given that  $\gamma$  is applied as the current control value, then,

$$\frac{1}{N_p} \sum_{j=1}^{N_p} I(C_k(\gamma, \delta_j(\gamma))) = 1 \quad (59)$$

where  $N_p$  is the number of evader particles. In this case, since all evader particles are reachable by the pursuer, it is obvious that the miss-set inclusion condition posed by Theorem 3 is met. By repeating this procedure for all values of  $\gamma \in U^p(t_k)$ , it is possible to map  $\mathcal{U}_p^*(t_k)$ . Thus,

$$\mathcal{U}_p^*(t_k) = \left\{ \gamma \in U^p(t_k) \mid \frac{1}{N_p} \sum_{j=1}^{N_p} I(C_k(\gamma, \delta_j(\gamma))) = 1 \right\} \quad (60)$$

If  $\mathcal{U}_p^*(t_k) = \emptyset$ , the front procedure provides a method for finding the control value according to Proposition 1. Specifically, it gives a measure for the portion of the evader's miss-set that is reachable by the pursuer. That is,

$$P_{\hat{\mathcal{M}}_e(t_k)}(\hat{\mathcal{M}}_p^y(t_k)) \approx \frac{1}{N_p} \sum_{j=1}^{N_p} I(C_k(\gamma, \delta_j(\gamma))) \quad (61)$$

The procedure to find the admissible set consists of a simple grid search on the feasible control set, carried out at each time step. Each grid point provides a possible control function value  $\gamma$ , for which the procedure to evaluate if  $\gamma \in \mathcal{U}_p^*(t_k)$  is as follows:

- 1) Generate  $N_p$  particles to represent the current evader state. The evader state is generated according to the estimated conditional PDF of  $x^E(t_k) | \mathcal{Z}^E(t_k)$ .
- 2) Generate  $N_p$  possible evader control function input sets  $u^E(\tau)_{\tau=t \rightarrow \infty}$  according to the assumed probabilistic model of the evader control policy.
- 3) Generate  $m$  particles to represent the current pursuer feasible front.
- 4) For each of the  $m$  pursuer particles, generate a control set of the form

$$\{u_i^p\}_{i=k}^{\infty} = \{\gamma, \delta_j, \delta_j, \delta_j, \dots, \delta_j, \dots\}, \quad j = 1, \dots, m \quad (62)$$

where  $\delta_j$  are evenly distributed on  $U^p(t_k)$ , thus mapping the front, possibly in a grid manner. For example, in Fig. 3,  $m = 25$  and the pursuer particles create the front surface vertices depicted in the figure.

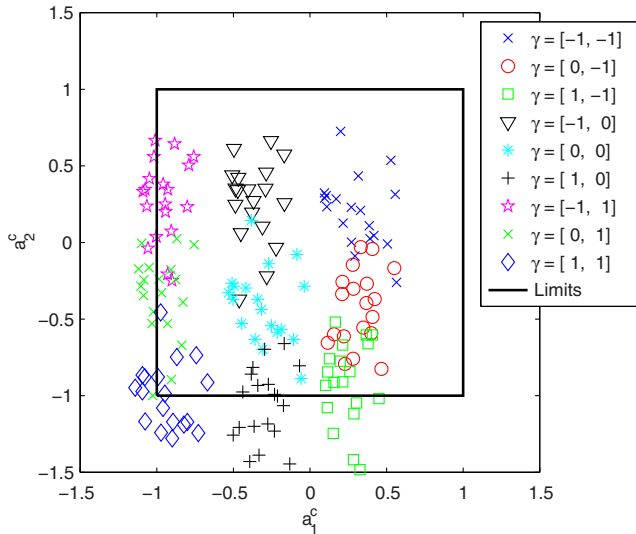


**Fig. 4** Mapping the time-invariant future control functions for various candidate control values  $\gamma$ . The control feasibility bounds are marked by the dark square.

5) Propagate both sets of particles in time using the system's equation of motion [Eq. (1)] until all evader particles intercept the pursuer front. It is assumed that the pursuer front extends linearly beyond the edge of feasible front and that any evader particles intercepting this extension indicate a miss.

6) Evaluate Eq. (60) and, when needed, Eq. (61).

In Fig. 4, the interception points on the front for all particles are displayed for various candidate current control function values. An interception point on the front is expressed by the pursuer time-invariant control function that will bring the pursuer to intercept that specific evader particle. As can be seen from Fig. 4, a nonuniqueness situation, as noted by Observation 3, occurs in this example, demonstrating the ability and need to introduce an additional constraint. This is the degree of freedom used, in what follows, to shape the pursuer's trajectory.

## B. Optimal Control Nonuniqueness

When  $\hat{\mathcal{M}}_p^u(t_k)$  is large enough to contain the set  $\hat{\mathcal{M}}_E(t_k)$ , it is obvious that the admissible set  $\mathcal{U}_p^*(t_k)$  will include more than one element. In such a case, an additional constraint is introduced in order to select a control value from the admissible set. Two such constraints are presented next.

### 1. Zero-Effort Evader Particle Trajectory Shaping

Let the zero-effort evader particle (ZEP) be an evader particle propagated with zero input command from the evader's estimated state. Let the ZEP's trajectory impact location on the front  $\mathcal{F}_k(s, \gamma)$  be  $\kappa_{\text{ZEP}}(\gamma)$ . Let  $\delta_{\text{ZEP}}(\gamma)$  define a pursuer control policy  $\mathcal{C}_k(\gamma, \delta_{\text{ZEP}}(\gamma))$  that guides the pursuer to hit  $\kappa_{\text{ZEP}}(\gamma)$ .

The following additional constraint is proposed:

$$u_k^P = \arg \min_{\gamma \in \mathcal{U}_p^*(t_k)} \|\delta_{\text{ZEP}}(\gamma)\|_2 \quad (63)$$

Notice that the pursuer trajectory resulting from control policy  $\mathcal{C}_k(\gamma, 0)$  describes the pursuer's zero-effort trajectory starting at the next time step. Thus,  $\delta_{\text{ZEP}}(\gamma) = 0$  implies that applying  $\gamma$  as the current pursuer control function value will position the pursuer at the next time step on a zero-effort trajectory that intercepts the evader's ZEP trajectory. Adopting the terminology used in differential game-based guidance laws,  $\delta_{\text{ZEP}}(\gamma) = 0$  implies that the zero-effort miss (ZEM) distance at the next time step will be zero. As such, when  $\mathcal{U}_p^*(t_k) = \mathcal{U}^P(t_k)$ , the resulting guidance law resembles the differential game guidance law with first-order dynamics, termed in [4] DGL/1. But, when  $\mathcal{U}^P(t_k) \setminus \mathcal{U}_p^*(t_k) \neq \emptyset$ , the resulting guidance law differs from the DGL/1 law because the actual pursuer command

that would render a zero ZEM may not be admissible by the miss-set inclusion theorem (Theorem 3). We term this proposed guidance law zero-effort evader particle trajectory shaping, and we use the shorthand notation ZTS in the ensuing.

### 2. Observability-Enhancing Trajectory Shaping

We propose to choose from the admissible set  $\mathcal{U}_p^*(t_k)$  the control function that will improve the observability of the evader's state by the pursuer's measurements. This is done by selecting from  $\mathcal{U}_p^*(t_k)$  the control function that maximizes the expected Fisher information matrix (FIM) in the next time step. Adopting the FIM measure from [29], we have

$$u_k^P = \arg \max_{\gamma \in \mathcal{U}_p^*(t_k)} \det l_\gamma(t_{k+1}) \quad (64)$$

where  $l_\gamma(t_{k+1})$  is the FIM evaluated at one time step into the future, i.e.,

$$l_\gamma(t_{k+1}) = \mathbb{E} \left[ \left[ \frac{\partial}{\partial \theta} \ln p_{\zeta_{k+1}}(\zeta_{k+1} | \hat{x}_{k+1}^E, x_{k+1}^P) \right] \times \left[ \frac{\partial}{\partial \theta} \ln p_{\zeta_{k+1}}(\zeta_{k+1} | \hat{x}_{k+1}^E, x_{k+1}^P) \right]^T \right] \quad (65)$$

where  $\zeta_{k+1}$  and  $p_{\zeta_{k+1}}$  are the measurement vector and PDF, respectively;  $\theta$  is the vector of evader state components for which we wish to improve the observability;  $x_{k+1}^P$  is the pursuer state propagated one step forward assuming that  $\gamma$  is the current control function value; and  $\hat{x}_{k+1}^E$  is the estimated evader's state. All these variables are assessed from the particles used in the procedure to determine  $\mathcal{U}_p^*(t_k)$ , described previously. We term this proposed guidance law observability-enhancing trajectory shaping, and use the shorthand notation OTS in the ensuing.

In a situation where heading toward the evader will result in an observability problem for the pursuer, OTS will choose to maneuver away. It will continue to do so until the evader's miss-set edge is tangent to the pursuer's miss-set, at which point OTS will need to start maneuvering back toward the evader in order to comply with Theorem 3 for as long as possible.

## VII. Simulation Study: Performance, Robustness, and Computational Aspects

A simulation study is presented to indicate the expected gain from the proposed OTS and ZTS approaches and to demonstrate their viability. The proposed approaches are compared with the perfect-information-based DGL/1 guidance law. The section also addresses the issue of performance robustness with respect to parameter uncertainties, as well as computational aspects (efficiency and accuracy) involved with real-time implementation.

### A. Scenario Description

The example consists of a highly nonlinear 3-D engagement scenario in which a pursuer having first-order delay dynamics engages an evader. Both the pursuer and evader maintain constant speeds; thus, their acceleration commands are perpendicular to their current velocities. The pursuer maximal acceleration is  $a_{\text{max}}^P = 60$  g, whereas the evader maximal acceleration is  $a_{\text{max}}^E = 20$  g. The acceleration time constants of both the pursuer and evader are  $\tau^P = \tau^E = 0.2$  s, respectively. The evader does not estimate the pursuer's state but is aware of the pursuer at the beginning of the game (in the present study, all engagements start at the beginning of the simulation). Thus, it applies a random bang-bang evasion maneuver that is known to be optimal for a blind target (see [14]).

The numerical study consists of two scenarios: 1) a head-on engagement, and 2) a flyby engagement. In the head-on engagement, the initial range between the pursuer and the evader is 10.8 km and the pursuer and evader speeds are 1500 and 1200 m/s, respectively, amounting to a nominal engagement time of 4 s. The flyby engagement situates the pursuer in an initial course that will cross (intercept) perpendicularly the evader's initial path with the same

nominal engagement time of 4 s. For a flyby engagement, [30] notes that, with a bearing-rate-only measurement, the target maneuver observability is minimal. Since our range measurement quality is poor, we may expect observability issues in the flyby engagement.

Two coordinate systems are defined: an inertial system, where the origin and axis directions are arbitrarily selected; and a pursuer body system. The body system's origin is located at the pursuer center of gravity, with its  $x$  axis pointing along the current pursuer velocity vector, its  $z$  axis pointing down, and its  $y$  axis completing a right-hand-rule system. The pursuer's initial motion direction is set on a collision course with the evader's initial location and velocity.

The pursuer dynamics is given using quaternion representation; thus, the pursuer state

$$x^P \triangleq [X^P, Y^P, Z^P, q^P, a_q^P, a_r^P]^T \quad (66)$$

is composed of its inertial position coordinates, a rotation quaternion  $q^P \triangleq [\lambda^P, \rho_x^P, \rho_y^P, \rho_z^P]^T$  specifying the rotation from the inertial reference frame to the body system, and its pitch and yaw accelerations, respectively. The pursuer's equations of motion are

$$\begin{bmatrix} \dot{X}^P \\ \dot{Y}^P \\ \dot{Z}^P \end{bmatrix} = \begin{bmatrix} \lambda^2 + \rho_x^2 - \rho_y^2 - \rho_z^2 \\ 2(\rho_x \rho_y - \lambda \rho_z) \\ 2(\rho_x \rho_z + \lambda \rho_y) \end{bmatrix} \|V^P\| \quad (67a)$$

$$\begin{bmatrix} \dot{\lambda}^P \\ \dot{\rho}_x^P \\ \dot{\rho}_y^P \\ \dot{\rho}_z^P \end{bmatrix} = \frac{1}{2\|V^P\|} \begin{bmatrix} 0 & 0 & -a_q^P & -a_r^P \\ 0 & 0 & -a_r^P & a_q^P \\ a_q^P & a_r^P & 0 & 0 \\ a_r^P & -a_q^P & 0 & 0 \end{bmatrix} \begin{bmatrix} \lambda^P \\ \rho_x^P \\ \rho_y^P \\ \rho_z^P \end{bmatrix} \quad (67b)$$

$$\begin{bmatrix} \dot{a}_q^P \\ \dot{a}_r^P \end{bmatrix} = -\frac{1}{\tau^P} \begin{bmatrix} a_q^P \\ a_r^P \end{bmatrix} + \frac{1}{\tau^P} u^P \quad (67c)$$

where  $V^P$  is the current pursuer velocity, and  $u^P \triangleq [a_c^P, a_r^P]^T$  is the (bounded) pursuer command vector ( $\|a_c^P\| \leq a_{\max}^P$  and  $\|a_r^P\| \leq a_{\max}^P$ ).

The evader state,  $x^E \triangleq [X^E, Y^E, Z^E, V_x^E, V_y^E, V_z^E, a_x^E, a_y^E]^T$ , is composed of its inertial position coordinates, velocity components, and pitch and yaw accelerations, respectively. The evader's EOM is

$$\dot{x}^E = \begin{bmatrix} 0_{3 \times 3} & I_{3 \times 3} & 0_{3 \times 1} \\ 0_{3 \times 3} & 0_{3 \times 3} & F_{ac}(x^E) \\ 0_{1 \times 3} & 0_{1 \times 3} & \frac{-1}{\tau^E} I_{2 \times 2} \end{bmatrix} x^E + \begin{bmatrix} 0_{6 \times 2} \\ \frac{1}{\tau^E} I_{2 \times 2} \end{bmatrix} u^E \quad (68)$$

where  $u^E \triangleq [a_c^E, a_r^E]^T$  is the (bounded) evader acceleration command vector perpendicular to its own velocity ( $\|a_c^E\| \leq a_{\max}^E$  and  $\|a_r^E\| \leq a_{\max}^E$ ),  $\tau^E$  is the evader's acceleration time constant, and  $F_{ac}(x^E)$  is given by

$$F_{ac}(x^E) = \frac{1}{\sqrt{V_x^E{}^2 + V_y^E{}^2}} \begin{bmatrix} \frac{V_x^E V_z^E}{\sqrt{(V_x^E{}^2 + V_y^E{}^2 + V_z^E{}^2)}} & -V_y^E \\ \frac{V_y^E V_z^E}{\sqrt{(V_x^E{}^2 + V_y^E{}^2 + V_z^E{}^2)}} & V_x^E \\ \frac{-(V_x^E + V_y^E)}{\sqrt{(V_x^E{}^2 + V_y^E{}^2 + V_z^E{}^2)}} & 0 \end{bmatrix} \quad (69)$$

The pursuer is modeled as having an imaging IR seeker providing the pursuer with a measurement of the line-of-sight (LOS) rates,  $\Lambda_1$  and  $\Lambda_2$ , and the relative range  $R$ . The LOS rate measurements are contaminated by an additive noise uniformly distributed on the interval  $[-0.1, 0.1]$  deg/s. The relative range measurement is contaminated by an additive noise uniformly distributed on  $[-10, 10]$  m.

The measurements are fed into an interacting multiple-model particle filter (IMM-PF) [11] that uses 1000 particles to estimate the evader state. The filter comprises four models (modes), with each describing an evader command option (e.g., "turning left and

upward"). The filter is aware of the evader's maximal acceleration capability and acceleration time constant. Using the estimated state and mode,  $N_p$  particles are selected and extrapolated forward in time in order to find their impact location on the pursuer front.

In the numerical example, the search procedure to find the admissible set  $\mathcal{U}_p^*(k)$  is implemented as a crude two-dimensional grid search, performed in each of the time steps of the 60 Hz rate guidance law computation (notice that the pursuer's acceleration time constant of 0.2 s amounts to an autopilot bandwidth of about 0.8 Hz). The grid points are  $[-1, 0, 1]a_{\max}^P$  for both acceleration commands. The Achilles heel of all SMC methods is the computer power that they demand, since a large number of simulations needs to be carried out. Although the proposed approach may be naturally implemented in a parallel computing environment, the required computational demands need to be taken into account. In light of this, the 1000 IMM-PF particles are resampled so that only  $N_p = 100$  particles are used to represent the evader and  $m = 25$  pursuer particles are used to represent the front for each grid point evaluation of  $\mathcal{U}_p^*(t_k)$ . A detailed discussion on computational aspects (serial vs parallel implementation and performance sensitivity as a function of computational power required) is given in a latter part of this section.

## B. Single-Run Analysis: Flyby Engagement

The trajectories of both the pursuer and evader in a single flyby engagement are shown in Fig. 5. Three different trajectories are shown for the pursuer, with each corresponding to a different active guidance law in the pursuer steering loop. For all three trajectories, all scenario random variables (namely, initial conditions, evader maneuvers, and measurement noises) are kept identical.

As shown in Fig. 5, the trajectory corresponding to the ZTS guidance law greatly resembles the one corresponding to the DGL/1 law (confirming the analysis of Sec. VI.B.1). Nevertheless, as seen in Table 1, DGL/1 achieves a miss distance of only 3.5 m, whereas ZTS reduces the miss distance to about 1.1 m. Observing the estimation errors at the end of the interception, also shown in Table 1, we see that the better performance of the ZTS guidance law (relative to that of the DGL/1 law) is achieved in spite of a significantly larger estimation error at the end of the game: 14.9 m for the ZTS law vs 0.8 m for the DGL/1 law. To understand these seemingly contradictory results, we turn to Figs. 6 and 7, which show the three position estimation errors (and associated standard deviation envelopes) as obtained in the runs depicted in Fig. 5 when the ZTS and DGL/1 guidance laws are active, respectively. Superimposed on these figures are the IMM-PF particle distributions, in each case, shown as histograms every 0.5 s. Recall that the pursuer is modeled as a first-order system with an acceleration time constant of 0.2 s. Due to this inherent delay, its achievable miss distance is mostly affected by the information provided to it by the estimator at about 1 s (five time constants) before impact. As can be seen from Figs. 6 and 7, for both guidance laws, at

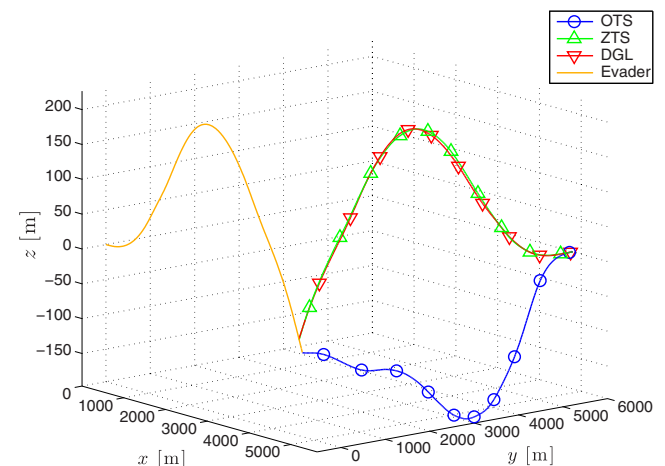


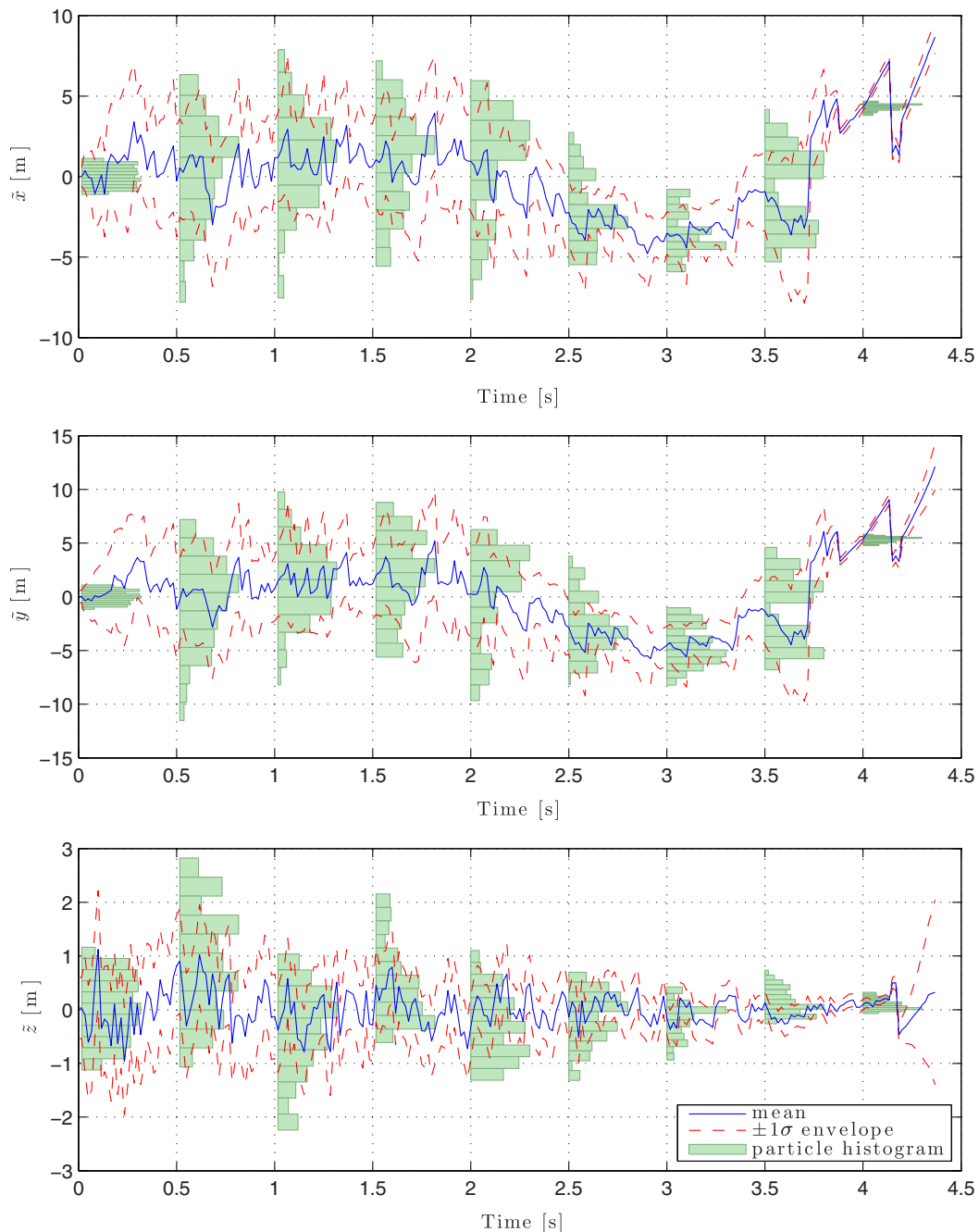
Fig. 5 Single run trajectories in a flyby engagement scenario.

**Table 1** Guidance laws performance in a flyby engagement (single run)

	Miss distance, m	Terminal estimation error, m
DGL/1	3.5	0.8
ZTS	1.1	14.9
OTS	0.7	0.1

about 1 s prior to impact, the estimator appears to yield two equally plausible estimates. This phenomenon, which is due to the poor observability characterizing this scenario, is manifested in the particle dual-peaked (and, thus, non-Gaussian) distributions observable at  $t = 3.5$  s. The ZTS guidance law attempts to hold all probable evader locations, as indicated by the distribution at that time, reachable for as long as possible (given its limited

maneuverability resources). By properly maneuvering to do that, it further sacrifices observability, which results in even larger estimation errors, but it maintains the target reachable and guides the pursuer toward the center of the evader's miss-set, which finally results in a relatively small miss distance. In a sense, the ZTS law maintains a proper balance between estimation performance (which is, obviously, not the main goal of the guidance loop) and interception performance (miss distance) while taking into account maneuverability constraints. In contradistinction, the DGL/1 guidance law does not account for estimation errors and treats the estimate as perfect information. When the estimate begins to diverge, at about  $t = 3.5$  s, the guidance law interprets this estimator divergence as an evasion maneuver and “greedily” steers the pursuer toward the (wrong) evader's position. By doing that, it does create a trajectory that enhances observability, which results in smaller estimation errors. However, the better estimation performance cannot be fully

**Fig. 6** IMM-PF position estimation error in flyby engagement (mean,  $\pm 1\sigma$  envelope, and particle histogram). ZTS guidance law.

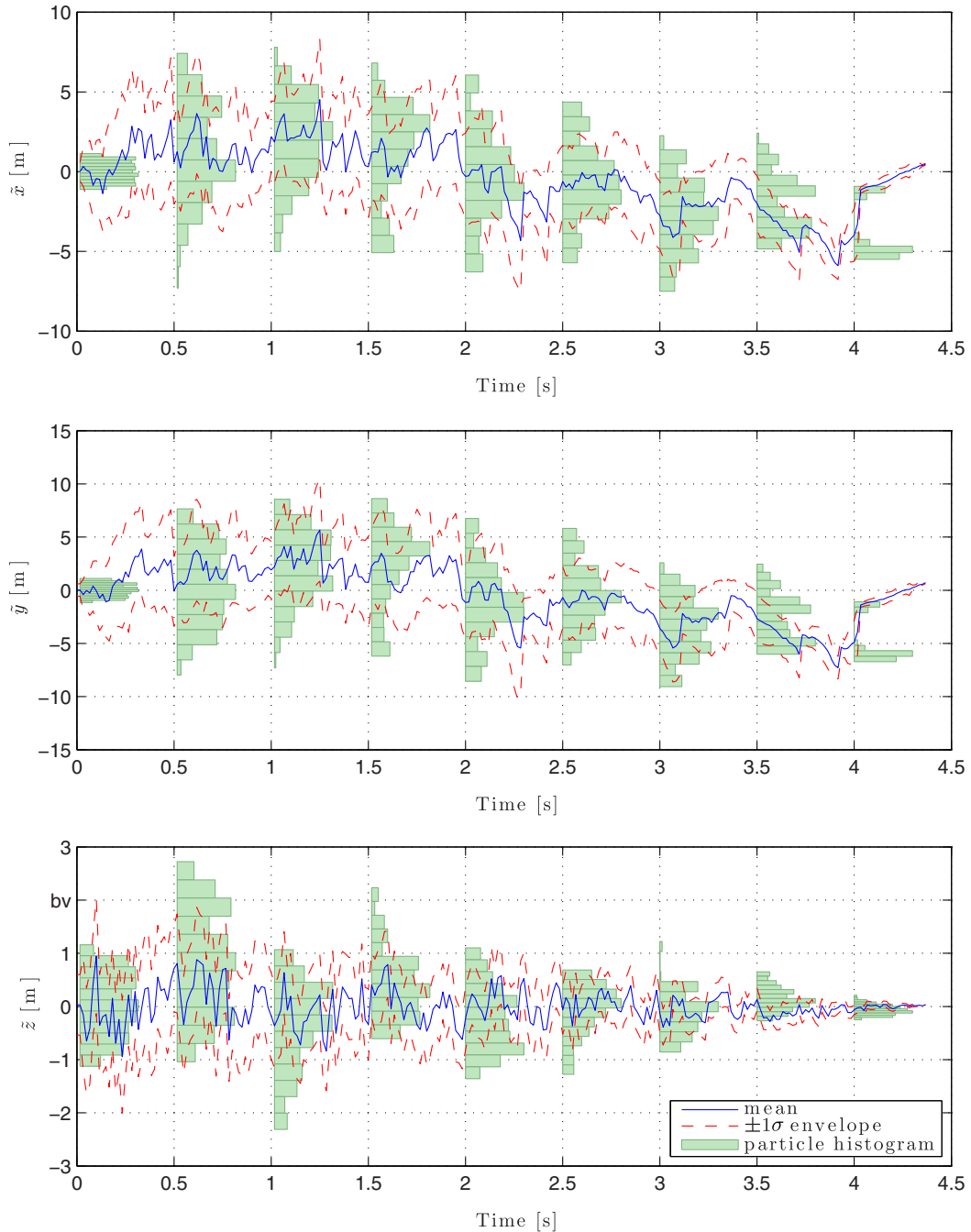


Fig. 7 IMM-PF position estimation error in flyby engagement (mean,  $\pm 1\sigma$  envelope, and particle histogram). DGL/1 guidance law.

exploited by the pursuer because it arrives too late (given the pursuer's inherent dynamic delay), and the resulting miss distance is more than three times larger than that of the ZTS-guided pursuer.

The OTS guidance law renders a distinctly different trajectory, as can be seen from Fig. 5. In this example, the OTS achieves a miss distance of about 0.7 m. The estimation performance of the particle filter with OTS in the loop is presented in Fig. 8. As can be seen from this figure, the estimation error is almost nullified within the final 1 s before impact.

### C. Monte Carlo Analysis

A Monte Carlo (MC) simulation study is carried out to test the performance of the proposed guidance law. In each simulation, all simulated measurement noise histories are generated beforehand and replayed three times: each time with a different guidance law in the loop. The MC study consists of 1000 such simulation sets.

Figures 9 and 10 show the cumulative distribution function (CDF) of the resulting miss distance for the head-on and flyby scenarios, respectively. By comparing the size of the warhead required to guarantee a kill with a given probability for each law, it can be concluded that both proposed laws outperform DGL/1. In the head-on scenario (Fig. 9), both ZTS and OTS require an effective warhead radius of about 0.4 m to guarantee an SSKP of 0.9, in comparison to an effective radius of about 1.0 m for the DGL/1 law. The performance of OTS resembles the performance of ZTS, indicating that there are no observability problems in a head-on engagement. In the flyby scenario (Fig. 10), in order to sustain an SSKP performance of 0.9, effective warhead radii of 0.5, 2.2, and 7.1 m for OTS, ZTS, and DGL/1, respectively, are required. Notice the severe degradation in DGL/1 performance due to the inherent uncertainty accompanying the evader's state. In the proposed approach, this uncertainty is addressed twice: first when calculating the guidance command, and

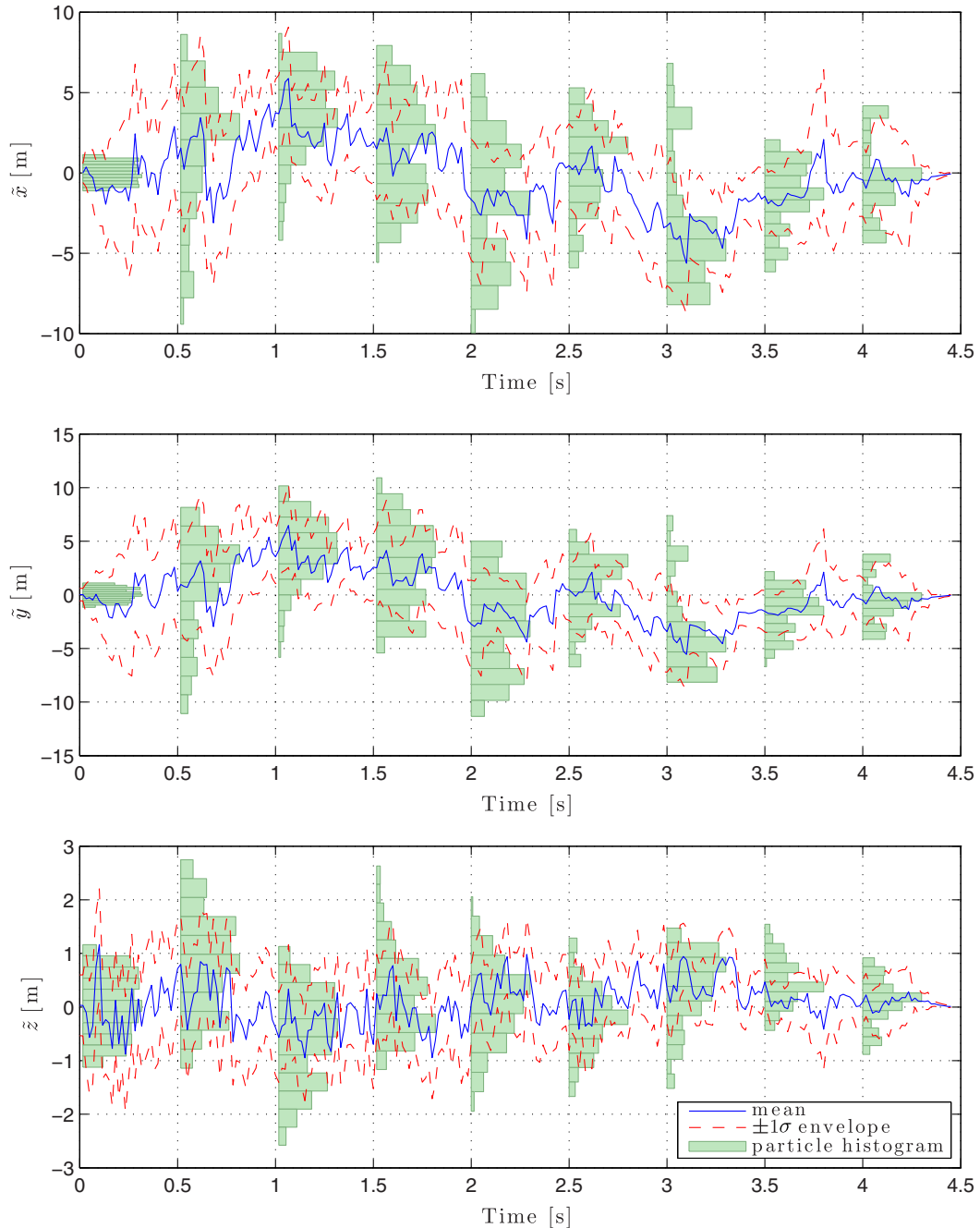


Fig. 8 IMM-PF position estimation error in flyby engagement (mean,  $\pm 1\sigma$  envelope, and particle histogram). OTS guidance law.

second by actively maneuvering to minimize this uncertainty through the creation of a favorable engagement geometry. ZTS addresses only the former issue, whereas OTS addresses both issues, thus boasting the superior performance exhibited in Fig. 10.

#### D. Sensitivity to Parameter Uncertainty

Thus far we have assumed, as is commonplace in the literature [24–26], that the evader’s acceleration time constant and acceleration bound are known to the pursuer. This information is required by the pursuer for 1) estimating the evader state (via the IMM-PF), and 2) estimating the evader’s miss-set. Obviously, in real life, this information is not readily available to the pursuer. However, it should be safe to assume that the pursuer possesses information on the bounded intervals within which both parameters should lie. Selecting values from these intervals will affect the pursuer’s estimate of the evader’s miss-set. Thus, it is reasonable for the pursuer to adopt a conservative approach and assume that the evader has a smaller time

constant and a larger acceleration limit (i.e., that the evader is, most likely, more agile than it really is). This assumption will render the pursuer’s estimate of the miss-set equal to or larger than the actual evader miss-set.

To evaluate the performance of the proposed approaches in the presence of parameter variations, we introduce uncertainties to the example used in the previous subsection. The uncertainties are listed in Table 2. For each of the 1000 MC runs, appropriate values for the evader’s true parameters are uniformly selected from these ranges. The pursuer adopts the conservative approach described herein and uses the values  $\tau^E = 0.1$  s and  $a_{\max}^E = 25$  g for miss-set estimation. As in the previous example, it has  $\tau^P = 0.2$  s and  $a_{\max}^P = 60$  g. Figures 11 and 12 present the results of 1000 MC runs for the head-on and flyby engagement geometry configurations, respectively. In comparison with Figs. 9 and 10, we see that, in the presence of model parameter uncertainties, the proposed guidance laws maintain performance integrity, exhibiting a graceful performance degradation.

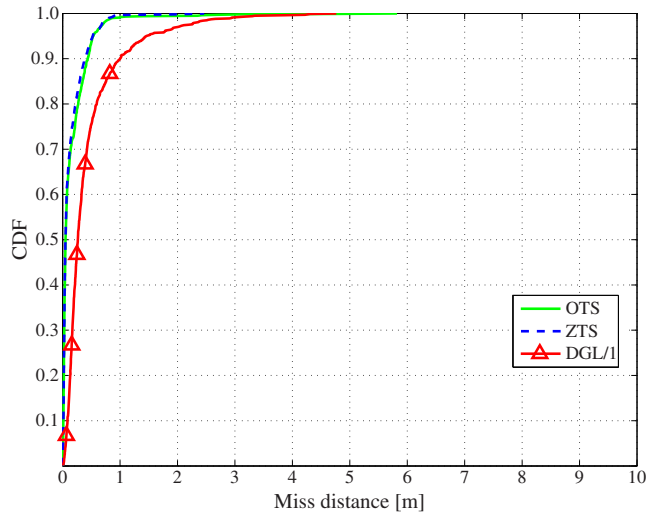


Fig. 9 Miss distance CDF in a head-on scenario.

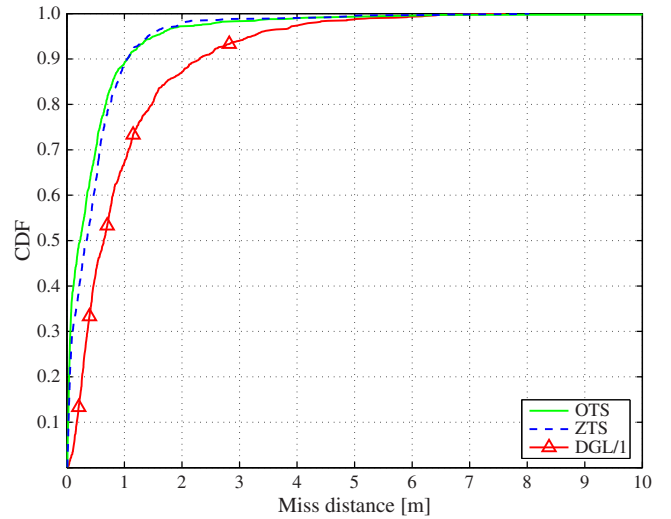


Fig. 11 Miss distance CDF in a head-on engagement with model uncertainties.

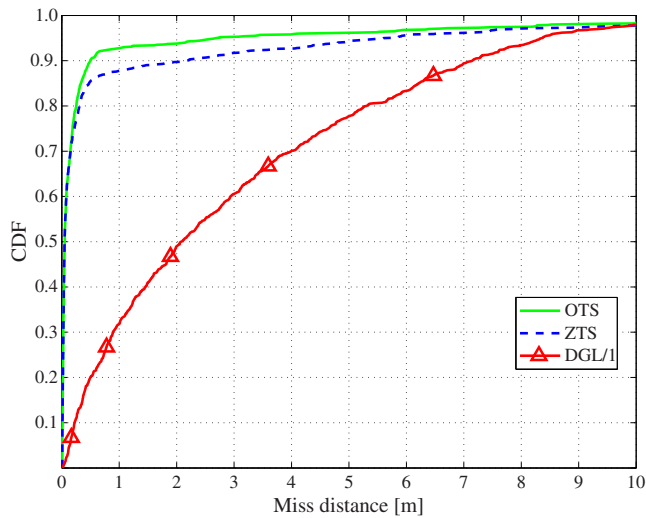


Fig. 10 Miss distance CDF in a flyby scenario.

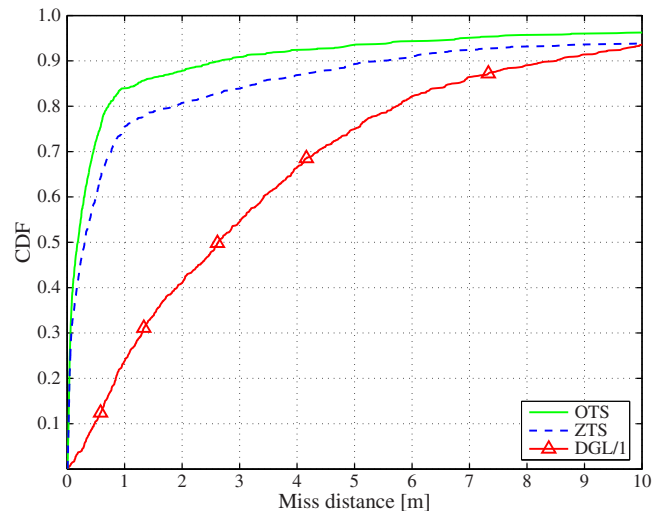


Fig. 12 Miss distance CDF in a flyby engagement with model uncertainties.

### E. Runtime Analysis

Any SMC-based computational method naturally gives rise to questions regarding the required computational power and the method's implementability in real-time applications. Our proposed approach is no exception, and the problem is even further compounded by the fact that the scenario on hand is a high-speed interception scenario characterized by a typical duration of a few seconds. It is, therefore, of interest to assess the computational requirements of the method, in order to be able to make some statements regarding real-life real-time implementability.

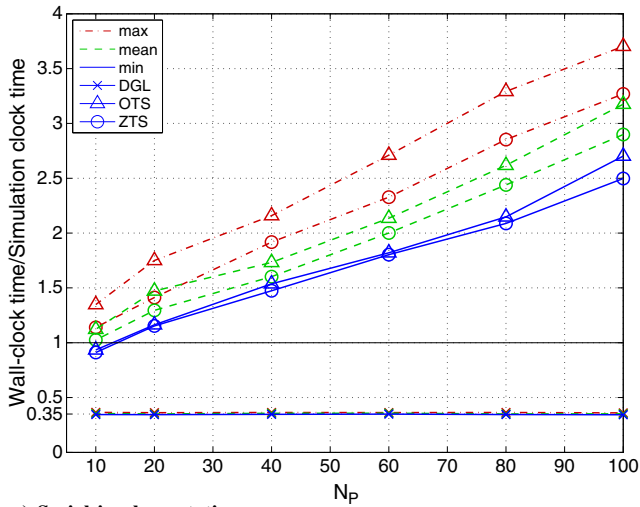
We checked runtime performance in the flyby engagement scenario using a consumer-grade Mac Pro computer, equipped with a single 12-Core Intel Xeon E5 CPU running at 2.7 GHz and using a non-real-time-compliant operating system. The simulation was first written (by a nonprofessional programmer) as a serial code in MATLAB 2009/Simulink, with the following three elements implemented in C and interfaced with MATLAB through the MATLAB MEX mechanism: 1) the IMM-PF evaluation, 2) the front procedure [analyzing if a given control function is admissible, i.e., if  $\gamma \in \mathcal{U}_p^*(t_k)$ ; Eq. (60)]; and, in the OTS case, 3) the FIM calculation; Eq. (65).

Table 2 Parameter uncertainty ranges

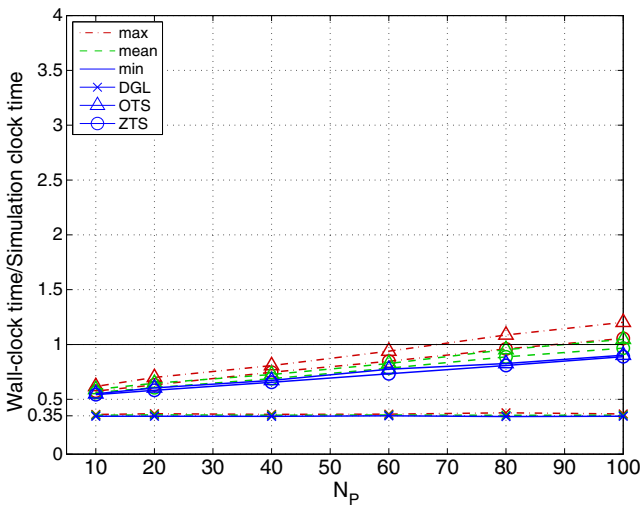
Parameter	Uncertainty range
Acceleration time constant $\tau^E$ , s	0.1–0.3
Acceleration bound $a_{\max}^E$ , g	15–25

Computed using 1000 MC runs, Fig. 13a presents the code runtime performance as a function of  $N_p$ , which is the number of evader particles used in the front computation procedure. The IMM-PF is implemented with a fixed number of 1000 particles. Code runtime performance is measured by its runtime factor, defined as the ratio of “wall clock” time to “simulation clock” time. As Fig. 13a shows, the serial code is not real-time compatible, as its runtime factor is greater than one (this threshold is shown in the figure as a horizontal black line). Nevertheless, a runtime factor value of about three (on average), obtained in the described environment, serves as a good indication that much can be done to bring it below the real-time threshold in a professional environment (featuring, e.g., professional programming, a real-time operating system, and dedicated real-time hardware). In particular, we note that, as is well known, SMC methods are highly amenable to parallel computation that, in a real-life application, would mean mechanization in a multiprocessor environment.

To roughly evaluate the computation speed enhancement potential of parallel implementation of the proposed method, we made an initial naive attempt at parallelizing the code by using the OpenMP v2.5 utility [31]. The simulation was rewritten (by a nonprofessional programmer) to get the front-procedure code running on 9 (out of the 12 available) cores our test computer provided. Only the front-procedure code was parallelized; all other elements in the simulation



a) Serial implementation



b) Parallel implementation (nine cores)

**Fig. 13** Runtime factor vs  $N_p$  (IMM-PF fixed at 1000 particles): minimum, maximum, and average times. 1000-run MC study using OTS, ZTS and DGL/1 guidance laws, flyby scenario.

remained in a serial configuration. Figure 13b presents the resulting parallel simulation runtime performance. As demonstrated, at  $N_p = 100$  our naive attempt at a parallel code implementation was almost sufficient to make the simulation run at real-time speeds, and a very minor reduction in the number of guidance particles got the simulation running faster than real-time. We note that, given the environment used to generate these numbers, it is obvious that these results should not be taken literally as the basis for practical algorithm design. The real message these results convey is that, adopting a professional approach to parallel SMC implementation (e.g., [32]), the new method should be real-time amenable using present-day technology.

#### F. Performance Versus Computational Load

As shown in Sec. VII.E, the computational load associated with the proposed algorithm grows roughly linearly with  $N_p$ , which is the number of evader particles used in the front procedure. A viable way to reduce the load is, therefore, to reduce  $N_p$ , which gives rise to a question regarding the sensitivity of the new method to  $N_p$ . To assess this sensitivity, we repeat the MC study of the flyby engagement scenario (the nominal results of which are shown in Fig. 10): this time varying  $N_p$ . In all MC runs, the number of particles used by the IMM-PF is fixed at 1000, whereas  $N_p \in \{10, 20, 60, 100\}$ .

Showing the miss distance CDF in each case, Figs. 14 and 15 depict the performance of the OTS and ZTS guidance laws,

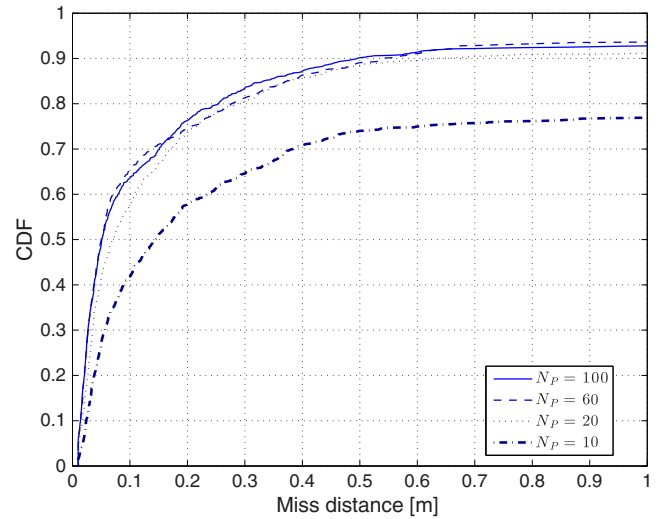


**Fig. 14** OTS miss distance performance vs  $N_p$  (IMM-PF fixed at 1000 particles), flyby scenario.

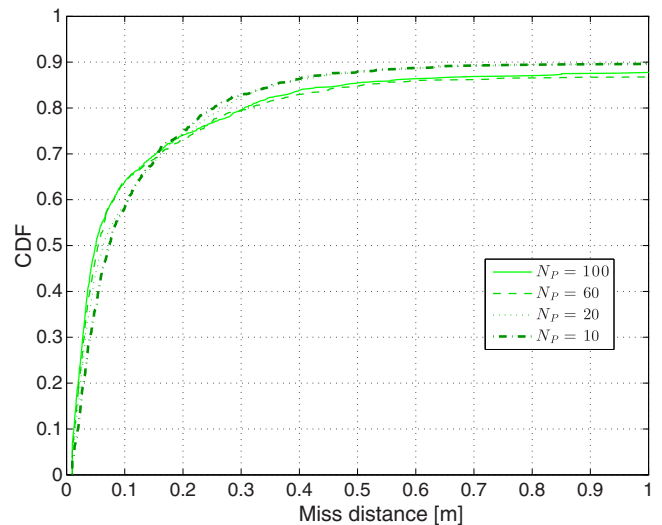


**Fig. 15** ZTS miss distance performance vs  $N_p$  (IMM-PF fixed at 1000 particles), flyby scenario.

respectively, as a function of  $N_p$ . As can be seen, the OTS law exhibits robust performance down to  $N_p = 20$  particles but suffers a severe performance deterioration at  $N_p = 10$  particles. In contrast, the performance of the ZTS law is insensitive to  $N_p$  within the tested range, as can be seen in Fig. 15. The sensitivity discrepancy between the OTS and ZTS guidance laws is rooted in the different goals that they strive to accomplish. The OTS law aims at estimating the miss-set region edges, which is a task that cannot be reliably done when the number of particles is reduced below a certain threshold. On the other hand, the ZTS law forgoes miss-set edge estimation, and it aims just at centering the evader's miss-set within the pursuer's miss-set, which is a less demanding task that can be accomplished with far fewer particles.

#### VIII. Conclusions

A novel approach to the problem of guidance in an uncertain scenario is presented. The new approach is compliant with the general separation theorem. Using a geometry-based approach, a perfect-information guidance law guaranteeing capture (in the deterministic sense) is formulated. This guidance law is based on the notion of miss-sets, which the pursuer has to estimate. When perfect information is not available, it is shown that a capture cannot be

guaranteed. However, the proposed approach demonstrates how the guidance law can accommodate estimation needs in order to minimize the miss distance. The performance of the proposed approach is compared to the performance of the DGL/1 guidance law, representing the best a player can do provided it has full and perfect information.

A simulation study is presented that demonstrates the viability of the proposed approach in a realistic, nonlinear non-Gaussian 3-D interception scenario. The study shows that a significant performance improvement can be achieved relative to an existing perfect-information differential-game-based law in the presence of partial information and non-Gaussian measurement noises. In addition, it is demonstrated that, in an imperfect-information scenario, the traditional head-on engagement is not the most challenging scenario.

The computational efficiency and accuracy of the method are explicitly addressed. Special attention to the IMM-PF implementation enables a mechanization with only 1000 particles to estimate the evader's full state. In addition, a crude proof-of-concept parallel implementation is used to convincingly demonstrate that the proposed approach can operate in real-time on present-day multiprocessor onboard computers. Furthermore, it is shown via simulations that, should real-time constraints limit the number of particles that can be used in the guidance scheme, the method exhibits exceptional robustness with respect to the number of particles.

Finally, it is noted that, in keeping with the state of the art, the pursuer is modeled as having full knowledge of the evader's acceleration time constant and maximal acceleration limit. When this knowledge is missing, it may be safely assumed that the pursuer knows, at least, interval bounds on these parameters. Adopting a conservative approach to the pursuer's construction of the evader's miss-set, the current extensive numerical simulations show that the sensitivity of the proposed method to uncertainties in these parameters is minor, and the method exhibits a graceful performance degradation as these uncertainties grow.

## Appendix A: Probability Space Construction

In this appendix, we show a possible construction for the probability space mentioned in Sec. IV. Recall that  $\Omega$  is  $\mathbb{R}^3 \times \mathbb{R}^+$  and  $\mathcal{F}$  is the  $\sigma$ -field of subsets of  $\Omega$ . We provide herein a procedure to construct a probability measure on  $\mathcal{F}$ ,  $P_{\hat{\mathcal{M}}_E(t)}$ , which is needed to defined the probability space  $(\Omega, \mathcal{F}, P_{\hat{\mathcal{M}}_E(t)})$ .

Define an evader particle  $\mathcal{P}^E$  as

$$\mathcal{P}^E \triangleq \{\hat{x}^E(t), u^E(\tau)_{\tau=t \rightarrow t_f}, w^E(\tau)_{\tau=t \rightarrow t_f}\} \quad (\text{A1})$$

where the conditional PDF of  $x^E(t)$  is  $p_{x^E(t)|Z^E(t)}$ ,  $u^E(\tau)_{\tau=t \rightarrow t_f}$  is an evader control function such that  $u^E(\tau) \in U^E(\tau) \forall \tau \in [t, t_f]$ , and  $w^E(\tau)_{\tau=t \rightarrow t_f}$  is a process noise sample function such that  $w^E(\tau) \sim p_{w^E} \forall \tau \in [t, t_f]$ . By the definition of  $\hat{\mathcal{R}}_E(t)$ , this particle describes an evader trajectory. Likewise, define a pursuer particle as

$$\mathcal{P}^P \triangleq \{x^P(t), u^P(\tau)_{\tau=t \rightarrow t_f}\} \quad (\text{A2})$$

where  $u^P(\tau)_{\tau=t \rightarrow t_f}$  is a pursuer control function such that  $u^P(\tau) \in U^P(\tau) \forall \tau \in [t, t_f]$ . Thus, by the definition of  $\mathcal{R}_P(t)$ , this particle describes a pursuer trajectory.

By Eq. (11), the terminal locations of the pursuer and evader, imposed by particles  $\mathcal{P}^P$  and  $\mathcal{P}^E$ , are found. Let  $\xi_P \in \Omega$  and  $\xi_E \in \Omega$  be these terminal locations, respectively. Notice that  $\xi_P$  is a point in  $\hat{\mathcal{M}}_P(t)$  and  $\xi_E$  is a point in  $\mathcal{M}_E(t)$ . Let  $d(a, b)$ ,  $a, b \in \Omega$ , be the conventional Euclidean distance on  $\Omega$ , and let  $\mathcal{B}_\epsilon(a)$ ,  $a \in \Omega$ , define an  $\epsilon$ -ball in  $\Omega$ :

$$\mathcal{B}_\epsilon(a) \triangleq \{\xi \in \Omega | d(\xi, a) < \epsilon\} \quad (\text{A3})$$

For a given  $\epsilon > 0$  and a threshold probability value  $0 < \Pi \ll 1$ , we can randomly generate  $N^E$  pairs of particles such that

$$N^E = \arg \min_N \left\{ \Pr \left[ \xi_E \notin \bigcup_{i=1}^N \mathcal{B}_\epsilon(\xi_E^i) \right] < \Pi \right\} \quad (\text{A4})$$

where  $\xi_E^i$  is an evader terminal location imposed by the  $i$ th pair of particles, and  $\xi_E$  is a possible evader terminal location.

Notice that the probability of generating a random pair of particles with an evader terminal point that is not coverable by

$$\bigcup_{i=1}^{N^E} \mathcal{B}_\epsilon(\xi_E^i)$$

is less than  $\Pi$ , which is a given small number. Furthermore, when  $p_{x_k^E|Z_k^E}$  has a bounded support, the set  $\hat{\mathcal{M}}_E$  is bounded. This may be deduced from the fact that  $U^E(t)$ ,  $U^P(t)$ , and  $W^E(t)$  are all bounded, rendering a bounded miss-set for a given initial state. If the initial state is distributed on a bounded support, then the union of all miss-sets generated by each of the initial states defined by the bounded support (i.e., the estimated miss-set [Eqs. (28) and (29)]), is also bounded. Since every bounded set in  $\mathbb{R}^n$  is compact, there is a finite cover for this set. Thus, if  $p_{x_k^E|Z_k^E}$  has a bounded support, then it is possible to have a finite value for  $N^E$  where  $\Pi = 0$  for any value  $\epsilon > 0$ .

Given  $\{\mathcal{B}_\epsilon(\xi_E^i)\}_{i=1}^{N^E}$  as defined previously, define a counting measure  $P_{\hat{\mathcal{M}}_E(t)}$  as follows:

$$P_{\hat{\mathcal{M}}_E(t)}(\mathcal{A}) \triangleq \frac{1}{N^E} \sum_{i=1}^{N^E} \mathcal{I}(\mathcal{A}, \mathcal{B}_\epsilon(\xi_E^i)) \quad \forall \mathcal{A} \in \mathcal{F} \quad (\text{A5})$$

where  $\mathcal{I}(\mathcal{A}, \mathcal{B})$  is an indicator function defined as

$$\mathcal{I}(\mathcal{A}, \mathcal{B}) = \begin{cases} 1 & \mathcal{B} \cap \mathcal{A} \neq \emptyset \\ 0 & \text{otherwise} \end{cases} \quad (\text{A6})$$

Notice that  $P_{\hat{\mathcal{M}}_E(t_k)}(\Omega) = 1$ ; hence,  $P_{\hat{\mathcal{M}}_E(t_k)}$  is a probability measure, rendering the triplet  $(\Omega, \mathcal{F}, P_{\hat{\mathcal{M}}_E(t_k)})$  a probability space.

## Appendix B: Proof of Lemma 1

*Proof:* The sets  $\mathcal{G}_1(t, s)$  and  $\mathcal{G}_2(t, s)$  are disjoint because

$$\begin{aligned} \mathcal{G}_1(t, s) \cap \hat{\mathcal{M}}_P^{u^P(s)}(s) &= \hat{\mathcal{M}}_E(t) \cap \mathcal{G}(s) \cap \hat{\mathcal{M}}_P^{u^P(s)}(s) \\ &= \hat{\mathcal{M}}_E(t) \cap (\hat{\mathcal{M}}_E(s) \setminus \hat{\mathcal{M}}_P^{u^P(s)}(s)) \cap \hat{\mathcal{M}}_P^{u^P(s)}(s) \\ &= \emptyset \end{aligned}$$

and

$$\begin{aligned} \mathcal{G}_2(t, s) \cap \hat{\mathcal{M}}_P^{u^P(s)}(s) &= \hat{\mathcal{M}}_E(t) \cap \{\hat{\mathcal{M}}_P^{u^P(s)}(s) \setminus \hat{\mathcal{M}}_P^{u^P(t)}(t)\} \cap \hat{\mathcal{M}}_P^{u^P(s)}(s) \\ &= \hat{\mathcal{M}}_E(t) \cap \{\hat{\mathcal{M}}_P^{u^P(s)}(s) \setminus \hat{\mathcal{M}}_P^{u^P(t)}(t)\} = \mathcal{G}_2(t, s) \end{aligned} \quad (\text{B1})$$

To see that  $\mathcal{G}_1(t, s)$  and  $\mathcal{G}_2(t, s)$  compose  $\mathcal{G}(t)$ , notice that

$$\begin{aligned} \mathcal{G}_1(t, s) \cup \mathcal{G}_2(t, s) &= (\hat{\mathcal{M}}_E(t) \cap \mathcal{G}(s)) \\ &\cup (\hat{\mathcal{M}}_E(t) \cap \{\hat{\mathcal{M}}_P^{u^P(s)}(s) \setminus \hat{\mathcal{M}}_P^{u^P(t)}(t)\}) \\ &= (\hat{\mathcal{M}}_E(t) \cap (\hat{\mathcal{M}}_E(s) \setminus \hat{\mathcal{M}}_P^{u^P(s)}(s))) \\ &\cup (\hat{\mathcal{M}}_E(t) \cap \{\hat{\mathcal{M}}_P^{u^P(s)}(s) \setminus \hat{\mathcal{M}}_P^{u^P(t)}(t)\}) \end{aligned} \quad (\text{B2})$$

Recalling Observation 2 and analyzing the first term, we have  $\hat{\mathcal{M}}_E(t) \subset \hat{\mathcal{M}}_E(s)$ ; hence,

$$\begin{aligned} \hat{\mathcal{M}}_E(t) \cap (\hat{\mathcal{M}}_E(s) \setminus \hat{\mathcal{M}}_P^{u^P(s)}(s)) \\ = \hat{\mathcal{M}}_E(t) \setminus \hat{\mathcal{M}}_P^{u^P(s)}(s) = \hat{\mathcal{M}}_E(t) \cap \overline{\hat{\mathcal{M}}_P^{u^P(s)}(s)} \end{aligned} \quad (\text{B3})$$

where  $\bar{A}$  denotes the complementary set of set  $A$ . Substituting Eq. (B3) into Eq. (B2) yields

$$\begin{aligned}
\mathcal{G}_1(t, s) \cup \mathcal{G}_2(t, s) &= \\
&= (\hat{\mathcal{M}}_E(t) \cap \overline{\hat{\mathcal{M}}_P^{u^p(s)}(s)}) \cup (\hat{\mathcal{M}}_E(t) \cap \{\hat{\mathcal{M}}_P^{u^p(s)}(s) \setminus \hat{\mathcal{M}}_P^{u^p(t)}(t)\}) \\
&= (\hat{\mathcal{M}}_E(t) \cap \overline{\hat{\mathcal{M}}_P^{u^p(s)}(s)}) \cup (\hat{\mathcal{M}}_E(t) \cap \hat{\mathcal{M}}_P^{u^p(s)}(s) \cap \overline{\hat{\mathcal{M}}_P^{u^p(t)}(t)}) \\
&= \hat{\mathcal{M}}_E(t) \cap (\overline{\hat{\mathcal{M}}_P^{u^p(s)}(s)} \cup \hat{\mathcal{M}}_P^{u^p(s)}(s) \cap \overline{\hat{\mathcal{M}}_P^{u^p(t)}(t)}) \\
&= \hat{\mathcal{M}}_E(t) \cap \overline{\hat{\mathcal{M}}_P^{u^p(t)}(t)} = \hat{\mathcal{M}}_E(t) \setminus \hat{\mathcal{M}}_P^{u^p(t)}(t) = \mathcal{G}(t)
\end{aligned}$$

(B4)

□

### Acknowledgments

The authors wish to express their gratitude to the anonymous reviewers who, with their thoughtful comments and suggestions, helped improve this paper.

### References

- [1] Zarchan, P., *Tactical and Strategic Missile Guidance*, 2nd ed., Vol. 157, Progress in Astronautics and Aeronautics, AIAA, Washington, D.C., 1994, pp. 17–35.
- [2] Ben-Asher, J. Z., and Yaesh, I., *Advances in Missile Guidance Theory*, Vol. 180, Progress in Astronautics and Aeronautics, AIAA, Reston, VA, 1998, pp. 25–126.
- [3] Shinar, J., and Gutman, S., “Three-Dimensional Optimal Pursuit and Evasion with Bounded Control,” *IEEE Transactions on Automatic Control*, Vol. 25, No. 3, 1980, pp. 492–496. doi:10.1109/TAC.1980.1102372
- [4] Shinar, J., “Solution Techniques for Realistic Pursuit-Evasion Games,” *Advances in Control and Dynamic Systems*, Vol. 17, edited by Leondes, C. T., Academic Press, New York, 1981, pp. 63–124.
- [5] Shinar, J., and Shima, T., “Nonorthodox Guidance Law Development Approach for Intercepting Maneuvering Targets,” *Journal of Guidance, Control, and Dynamics*, Vol. 25, No. 4, 2002, pp. 658–666. doi:10.2514/2.4960
- [6] Oshman, Y., and Arad, D., “Differential-Game-Based Guidance Law Using Target Orientation Observations,” *IEEE Transactions on Aerospace and Electronic Systems*, Vol. 42, No. 1, Jan. 2006, pp. 316–326. doi:10.1109/TAES.2006.1603425
- [7] Shima, T., Shinar, J., and Weiss, H., “New Interceptor Guidance Law Integrating Time-Varying and Estimation-Delay Models,” *Journal of Guidance, Control, and Dynamics*, Vol. 26, No. 2, 2003, pp. 295–303. doi:10.2514/2.5046
- [8] Maybeck, P. S., *Stochastic Models, Estimation, and Control*, Vol. 25, Academic Press, New York, 1982, pp. 129–136, Chap. 10.8.
- [9] Blom, H. A., and Bar-Shalom, Y., “The Interacting Multiple Model Algorithm for Systems with Markovian Switching Coefficients,” *IEEE Transactions on Automatic Control*, Vol. 33, No. 8, Aug. 1988, pp. 780–783. doi:10.1109/9.1299
- [10] Chen, G., Wang, J., and Shieh, L., “Interval Kalman Filtering,” *IEEE Transactions on Aerospace and Electronic Systems*, Vol. 33, No. 1, Jan. 1997, pp. 250–259. doi:10.1109/7.570759
- [11] Doucet, A., De Freitas, N., and Gordon, N., *Sequential Monte Carlo Methods in Practice*, Statistics for Engineering and Information Science, Springer-Verlag, New York, 2001, pp. 17–73, 269–271.
- [12] Stengel, R. F., *Stochastic Optimal Control*, Wiley, New York, 1986, pp. 420–493.
- [13] Shinar, J., and Turetsky, V., “What Happens When the Certainty Equivalence Is Not Valid, Is There an Optimal Estimator for Terminal Guidance?” *Annual Reviews in Control*, Vol. 27, No. 2, 2003, pp. 119–130. doi:10.1016/j.arcontrol.2003.10.001
- [14] Shinar, J., Shima, T., and Kebke, A., “On the Validity of Linearized Analysis in the Interception of Reentry Vehicles,” *AIAA Guidance, Navigation, and Control Conference*, AIAA Paper 1998-4303, Aug. 1998, pp. 1050–1060.
- [15] Shinar, J., Turetsky, V., and Oshman, Y., “Integrated Estimation/Guidance Approach for Improved Homing Against Randomly Maneuvering Targets,” *Journal of Guidance, Control, and Dynamics*, Vol. 30, No. 1, 2007, pp. 154–161. doi:10.2514/1.22916
- [16] Witsenhausen, H. S., “Separation of Estimation and Control for Discrete Time Systems,” *Proceedings of the IEEE*, Vol. 59, No. 11, Nov. 1971, pp. 1557–1566. doi:10.1109/PROC.1971.8488
- [17] Hexner, G., Shima, T., and Weiss, H., “An LQG Guidance Law with Bounded Acceleration Command,” *Proceedings of the 42nd IEEE Conference on Decision and Control*, Vol. 1, IEEE Publ., Piscataway, NJ, 2003, pp. 715–720.
- [18] Hexner, G., and Shima, T., “Stochastic Optimal Control Guidance Law with Bounded Acceleration,” *Proceedings of the 43rd IEEE Conference on Decision and Control*, Vol. 3, IEEE Publ., Piscataway, NJ, 2004, pp. 3021–3026.
- [19] Dionne, D., Michalska, H., and Rabbath, C. A., “A Predictive Guidance Law with Uncertain Information About the Target State,” *American Control Conference*, IEEE Publ., Piscataway, NJ, June 2006, pp. 1062–1067. doi:10.1109/ACC.2006.1656357
- [20] Shaviv, I. G., and Oshman, Y., “Guidance Without Assuming Separation,” *AIAA Guidance, Navigation, and Control Conference*, AIAA Paper 2005-6154, Aug. 2005.
- [21] Shaviv, I. G., and Oshman, Y., “Fusion of Estimation and Guidance Using Sequential Monte Carlo Methods,” *Proceedings of IEEE Conference on Control Applications*, IEEE Publ., Piscataway, NJ, Aug. 2005, pp. 1361–1366.
- [22] Shaviv, I. G., and Oshman, Y., “Estimation-Guided Guidance,” *AIAA Guidance, Navigation, and Control Conference*, AIAA Paper 2006-6217, Aug. 2006.
- [23] Bertsekas, D. P., and Rhodes, I. B., “On the Minimax Reachability of Target Sets and Target Tubes,” *Automatica*, Vol. 7, No. 2, 1971, pp. 233–247. doi:10.1016/0005-1098(71)90066-5
- [24] Shima, T., Shinar, J., and Weiss, H., “New Interceptor Guidance Law Integrating Time-Varying and Estimation-Delay Models,” *Journal of Guidance, Control, and Dynamics*, Vol. 26, No. 2, March–April 2003, pp. 295–303. doi:10.2514/2.5046
- [25] Atir, R., Hexner, G., Weiss, H., and Shima, T., “Target Maneuver Adaptive Guidance Law for a Bounded Acceleration Missile,” *Journal of Guidance, Control, and Dynamics*, Vol. 33, No. 3, May–June 2010, pp. 695–706. doi:10.2514/1.47276
- [26] Shima, T., Oshman, Y., and Shinar, J., “Efficient Multiple Model Adaptive Estimation in Ballistic Missile Interception Scenarios,” *Journal of Guidance, Control, and Dynamics*, Vol. 25, No. 4, 2002, pp. 667–675. doi:10.2514/2.4961
- [27] Forte, I., and Shinar, J., “Improved Guidance Law Design Based on the Mixed-Strategy Concept,” *Journal of Guidance, Control, and Dynamics*, Vol. 12, No. 5, 1989, pp. 739–745. doi:10.2514/3.20469
- [28] Lawrence, R. V., “Interceptor Line-of-Sight Rate Steering: Necessary Conditions for a Direct Hit,” *Journal of Guidance, Control, and Dynamics*, Vol. 21, No. 3, May–June 1998, pp. 471–476. doi:10.2514/2.4260
- [29] Oshman, Y., and Davidson, P., “Optimization of Observer Trajectories for Bearings-Only Target Localization,” *IEEE Transactions on Aerospace and Electronic Systems*, Vol. 35, No. 3, July 1999, pp. 892–902. doi:10.1109/7.784059
- [30] Hepner, S. A., and Geering, H. P., “On the Observability of Target Maneuvers via Bearing-Only and Bearing-Rate-Only Measurements,” *AIAA Guidance, Navigation, and Control Conference*, AIAA Paper 1987-2382, Aug. 1987, pp. 560–569.
- [31] Chapman, B., Jost, G., and van der Pas, R., *Using OpenMP: Portable Shared Memory Parallel Programming*, The MIT Press, Cambridge, MA, 2007, [https://mitpress.mit.edu/sites/default/files/titles/content/9780262533027\\_sch\\_0001.pdf](https://mitpress.mit.edu/sites/default/files/titles/content/9780262533027_sch_0001.pdf).
- [32] Zhou, Y., “vSMC: Parallel Sequential Monte Carlo in C++,” *Journal of Statistical Software*, Vol. 62, No. 9, Jan. 2015, pp. 1–49. doi:10.18637/jss.v062.i09